Petroleum Science 21 (2024) 1149–1170

Contents lists available at ScienceDirect

Petroleum Science

journal homepage: www.keaipublishing.com/en/journals/petroleum-science

Original Paper

Simulation study on cuttings transport of the backreaming operation for long horizontal section wells

Yu-Fei Chen [a], Hui Zhang [a, *], Wen-Xin Wu [b], Jun Li [a], Yong Ouyang [c], Zong-Yu Lu [d], De-Xin Ma [e], Yong-Chuan Wu [e], Jun-Bo Liu [e], Ke-Rou Liu [a], Zhuo-Xin Dong [a]

[a] China University of Petroleum (Beijing), Beijing, 102249, China
[b] Beijing Normal University at Zhuhai, Experimental and Practical Education Innovation Center, Zhuhai, 519087, Guangdong, China
[c] Oil & Gas Technology Research Institute of PetroChina Changqing Oilfield Company, Xi'an, 710016, Shaanxi, China
[d] PetroChina Xinjiang Oilfield Company, Karamay, 834002, Xinjiang, China
[e] China Oilfield Services Ltd., Tianjin, 300459, China

ARTICLE INFO

Article history:
Received 4 January 2023
Received in revised form
22 September 2023
Accepted 24 September 2023
Available online 26 September 2023

Edited by Jia-Jia Fei

Keywords:
Backreaming
Stuck pipe
Hole cleaning
Transient solid transport
Multiple flow patterns

ABSTRACT

The backreaming operation plays a significant role in safe drilling for horizontal wellbores, while it may cause severe stuck pipe accidents. To lower the risk of the stuck pipe in backreaming operations, the mechanism of cuttings transport needs to be carefully investigated. In this research, a transient cuttings transport with multiple flow patterns model is developed to predict the evolution of cuttings transported in the annulus while backreaming. The established model can provide predictions of the distribution of cuttings bed along the wellbore considering the bulldozer effect caused by large-size drilling tools (LSDTs). The sensitivity analyses of the size of LSDTs, and backreaming operating parameters are conducted in Section 4. And a new theory is proposed to explain the mechanism of cuttings transport in the backreaming operation, in which both the bit and LSDTs have the "cleaning effect" and "plugging effect". The results demonstrate that the cuttings bed in annuli is in a state of dynamic equilibrium, but the overall trend and the distribution pattern are obvious. First, larger diameters and longer drilling tools could lead to a higher risk of the stuck pipe. Second, we find that it is not the case that the higher flow rate is always better for hole cleaning, so three flow-rate intervals are discussed separately under the given conditions. When the "dangerous flow rate" (<33 L/s in Case 4) is employed, the cuttings bed completely blocks the borehole near the step surface and causes a stuck pipe directly. If the flow rate increases to the "low flow rate" interval (33–35 L/s in Case 4), a smaller flow rate instead facilitates borehole cleaning. If the flow rate is large enough to be in the "high flow rate" interval (>35 L/s in Case 4), the higher the flow rate, the better the cleaning effect of cuttings beds. Third, an interval of tripping velocity called "dangerous velocity" is proposed, in which the cuttings bed accumulation near the LSDTs is more serious than those of other tripping velocities. As long as the applied tripping velocity is not within the "dangerous velocity" (0.4–0.5 m/s in Case 5) interval in the backreaming operation, the risk of the stuck pipe can be controlled validly. Finally, through the factors analyses of the annular geometry, particle properties, and fluid properties in Section 5, it can be found that the "low flow rate", "high flow rate" and "dangers flow rate" tend to decrease and the "dangerous velocity" tends to increase with the conditions more favorable for hole cleaning. This study has some guiding significance for risk prediction and parameter setting of the backreaming operation.

1. Introduction

Considering the top-drive drilling system is popular in drilling engineering, the operation of backreaming is an essential technique in the construction of horizontal wellbores (Yarim et al., 2010). With the length of the horizontal section increasing, the risk of

* Corresponding author.
E-mail address: zhanghuicup@outlook.com (H. Zhang).

https://doi.org/10.1016/j.petsci.2023.09.021

Nomenclature

A_{sb}	the cross-section area of the solid bed layer, m^2
A_{sd}	the cross-section area of the suspension layer, m^2
C_c	the cuttings concentration, dimensionless
C_D	the drag coefficient
C_f	the fluid concentration, dimensionless
C_{sb}	the solid concentration of the solid bed layer, dimensionless
D_{hy}	the hydraulic radius, m
d_c	the diameter of a particle, m
d_o	the outer diameter of the pipe, m
d_i	the inner diameter of the pipe, m
d_{lsdt}	the outer diameter of the large-size drilling tool, m
e_c	the eccentric distance, m
e	the eccentricity, $e = \frac{2e_c}{d_o - d_i}$, dimensionless
F	the dry friction force, N
F_{cf}	multiparticle-drag force, N
g	the acceleration of gravity, m/s^2
h_c	the cuttings bed height, m
h_d	the dimensionless cuttings bed height, $h_d = h_c/d_o \times 100$, %
$h_{d,aver}$	the average dimensionless cuttings bed height of the section from 0 to 20 m (and 0–40 m) from the LSDT, %
$h_{d,max}$	the maximum dimensionless cuttings bed height, %
K	the consistency coefficient, $Pa \cdot s^n$
L_{har}	the length of the hazardous section, m
L_{br}	the backreaming distance, m
S_{sd}	the wetted perimeter of the suspension layer, m
S_{sb}	the wetted perimeter of the bed layer, m
S_{sbsd}	the wetted perimeter of the interface, m
u_{ter}	the terminal velocity of a particle, m/s
v_f	the velocity of the liquid phase in the suspension layer, m/s
v_{fr}	the modified velocity of the liquid phase, m/s
v_c	the velocity of the solid phase in the suspension layer, m/s
v_{sb}	the velocity of the solid bed layer, m/s
v_{br}	the tripping velocity, m/s
v_a	the angular velocity, m/s
V_{mb}	the volume of cuttings bed migration, m^3
x	the length of trajectory from the bottom hole, m
ρ_f	the drilling mud density, kg/m^3
ρ_c	the cuttings density, kg/m^3
ρ_{sb}	the solid bed density, kg/m^3
θ	the inclination angle, radians
τ	the shear stress, Pa
τ_y	the yield stress, Pa
τ_{sbsd}	the shear stress for the interface between the suspension layer and solid layer, Pa
τ_{fw}	the shear stress for the interface between the liquid phase in the suspension layer and wall, Pa
τ_{sbw}	the shear stress for the interface between the bed layer and wall, Pa
τ_{cw}	the shear stress for the interface between the solid phase in the suspension layer and wall, Pa
γ	the shear rate, 1/s
Φ_{sdc}	the mass flux of solid in the suspension layer, $kg/(s \cdot m)$
Φ_{sdf}	the mass flux liquid in the suspension layer, $kg/(s \cdot m)$
Φ_{sb}	the mass flux of the bed layer, $kg/(s \cdot m)$
ω_n	the angular velocity of the rotating drill pipe, rad/s
φ	repose angle, radians
Δt	the time step, s
Δx	the spatial step, m

backreaming operation becomes higher. A well in Ohio set the record for the longest inland horizontal well in the United States with a horizontal section of 5652.2m (Sun and Jia, 2020). A horizontal well with a horizontal section of 5060m has been completed in Changqing Oilfield setting a record for the longest horizontal section in China. As long horizontal wellbores are adopted more and more widely, backreaming as a key operation of tripping in horizontal sections should be emphasized and evaluated quantitatively.

The backreaming is a process of pulling the revolving drill pipe out of the borehole with the pump on, as shown in Fig. 1. According to some drill cases in China, the backreaming operations are integral parts of the tripping-out process. Generally, backreaming operations are developed to remove the cuttings bed and to trim the walls of the hole if necessary. However, when the backreaming is performed improperly, unintended consequences could be triggered, such as the stuck pipe and cavings, etc. (Yarim et al., 2010). During the process of the backreaming, a mass of cuttings near the rotating bit is resuspended and transferred, of which a portion is deposited as new cuttings bed in the upper intervals of the wellbore, as shown in Fig. 1. The cuttings-induced blockage caused by the backreaming account for about 65% of stuck-pipe accidents with Schlumberger's statistics (Yarim et al., 2007). During the process of the LSDTs pulled out of the borehole axially, there are cuttings pushed forward and deposited adjacent to the step surfaces. The LSDTs consisting of stabilizers, drill collars, and rotary steerable tools show larger diameters than drill strings (Tan and Zhang, 2022). From 2014 to 2019, oil fields in Sichuan and Chongqing suffered a loss of 45 sets of rotary steerable tools because of solid-settling-stuck incidents (Fan et al., 2020; Tan and Zhang, 2022). There is a serious solid-settling-stuck accident in the process of backreaming in the Weiyuan Oilfield in 2018, which lead to huge economic losses because of explosive releasing and sidetracking twice. To eliminate the side effects of backreaming, it is necessary to establish a new principle for backreaming operations of the time to begin, to slow down, and to stop, as well as the way to do it (Yarim et al., 2010; Zamora et al., 1993). In addition, the intervals of the wellbore with a medium inclination angle are more liable to avalanches (Zamora et al., 1993), and the backreaming would exacerbate this situation.

To date, quantitative risk assessment studies on backreaming operations are quite rare. In the past investigation, Tan and Zhang (2022) proposes the concept of the bulldozer effect to describe the phenomenon that the LSDT pushes forward cuttings axially in the horizontal section of a wellbore. The hook load, as well as the top drive torque, are calculated based on tubular mechanics theory when a cuttings cylinder appears in front of the bit under the condition of tripping out. It's only a matter of time before pipes get stuck if a cuttings cylinder appears (Tan and Zhang, 2022). The formation of a cuttings cylinder in the annulus is an uncommon and the worst situation. The process of accumulated cuttings forming dunes in the wellbore is usual and requires extra attention in comparison. Zhu et al. (2022) come up with a conclusion that the cuttings would accumulate near the stabilizer while tripping out. They believe the reason why the phenomenon appears is a

mutation of the flow velocity near the stabilizer without considering the bulldozer effect of the stabilizer. However, it cannot be neglected that the LSDT piling up cuttings is the main driver of the redistribution of cuttings. The bulldozer effect must be taken into account when simulating the backreaming process.

To deal with cutting-induced blockage problems, scholars have dedicated to figuring out the mechanism of cuttings transport in the wellbore through three major methods which are indoor experiments (Zhang, 2015; Naganawa et al., 2017; Khatibi et al., 2018; Tong et al., 2021a), numerical simulation with CFD software (Zhang, 2015; Epelle and Gerogiorgis, 2018; Zhang et al., 2020; Khaled et al., 2021), and one-dimension solid-liquid flow models. Considering the simulation of backreaming operations needs a very long annulus of the wellbore, both methods of experiments and CFD software have the disadvantage of high simulation costs. Generally, one-dimensional layer models are employed to simulate the evolution of cuttings with high-computational speed for a wild range of wellbore trajectories. The layer-model methods have been widely employed and studied, which is introduced into drilling engineering by Gavignet and Sobey (1989). This study has benefited from improvements in the layer models. Naganawa et al. (2017) proposed a new function of critical friction velocity based on the inclination angle and reposed angle. Zhu et al. (2021) applied buoyancy to the momentum equations and found that buoyancy has little effect on horizontal or close horizontal sections. Tong et al. (2021a) modified the entrainment factor and deposition factor and introduced the critical deposition velocity to the deposition mass flux. Chen et al. (2022) proposed a modified model of the mass exchange flux based on the critical rolling velocity of which results were more consistent with experimental observations. An et al. (2023) propose a correction factor to modify the model to obtain a more accurate pressure gradient.

The flow pattern of solids and liquids is assumed as either two-layer (Naganawa et al., 2017; Naganawa and Nomura, 2006) or three-layer (Zhang et al., 2018; Wang and Long, 2010) types for conventional models. However, the flow pattern of the cuttings and drilling fluid in annuli constantly changes during the actual flow process. The assumption of multiple flow patterns according to flow parameters in the simulation is more consistent with the experimental observations (Tong et al., 2021a; Wang, 2020; Zhang et al., 2018). In addition, flow patterns in different positions of the wellbore vary greatly, when the LSDT and excessive cuttings resuspended by the bit from the bottom hole are considered. If only one flow pattern in the annulus is assumed, it is very easy to have unexpected negative volume or negative velocity, which leads to the termination of the iteration. Thus, the assumption of multiple flow patterns must be employed in the simulation of backreaming operations with LSDTs.

In this paper, the transient solid transport model of one dimension with multiple flow patterns is developed to simulate the process of backreaming. The traditional model of one dimension cannot deal with the excessive dry friction caused by the concentrated distribution of cuttings. According to the characteristics of cuttings transport of the backreaming operation, five kinds of flow patterns are employed to modify the conventional model. The behaviors of cuttings transport while backreaming are explored with the following advantages and improvements: 1) Quantitative forecasts and factors analyses are developed based on the fluid mechanical model, revealing the mechanism of the cutting-induced blockage due to the backreaming operation and providing an objective basis for setting parameters; 2) With the dynamic meth method adopted, the boundary conditions for backreaming operations are proposed to simulate the axial motion of the bit, drilling pipes, and LSDTs; 3) The bulldozer effect caused by LSDTs in horizontal sections of the wellbore is introduced to the model. This work is accomplished and aimed to play a guiding role in the parameter settings of the backreaming operation on site.

2. Mechanism for the cutting transport during the backreaming operation

2.1. Backreaming process

Backreaming is considered similar to “drilling backward”, where the drill pipes are pulled out of the borehole and the pump turns on (Yarim et al., 2010). Compared to the drilling process, the area near the bit plays a more crucial role. In the backreaming process, the cuttings bed in the area near the bit directly determines the cuttings supply to the upper intervals of the wellbore. Excessive cuttings resuspended by the bit are deposited in the upper intervals, which may result in a blockage of the annulus. As shown in Fig. 2, the rotating bit stirs all cuttings bed in its place into the flow as suspended cuttings particles from the bottom of the conduit. The solids bed is cleaned successively with the axial advances of the bit while tripping out, which is called the “cleaning effect” of the bit in this paper. However, the cuttings particles would be deposited again at the lower side of the annulus by gravity after being transferred for a certain distance (Zhang et al., 2020). Generally, although the wellbore interval the bit passes through is clean, the upper interval of the wellbore gets more deposited cuttings, which is called the “plugging effect” of the bit in this study. The cleaning and plugging effects are consistent, and the more the bit clears the bed, the more cuttings are expected to be deposited in the upper interval. Therefore, the backreaming operation is a double-edged sword for hole cleaning. Which of the two effects of the bit is dominant in the backreaming operation depends on the tripping velocity, the LSDTs, and the flow rate. If the right combination of parameters is done, the bit would play a dominant role in cleaning the bottom hole, otherwise, the backreaming would be a disaster for hole cleaning.

2.2. Bulldozer effect

The LSDTs show greater outer diameters than the drill pipes (Tan and Zhang, 2022). The step surface is part of the cross-section of the drilling tool that projects relative to the drill string. A step surface normally exists at the joint of the drilling tool, where the diameter changes. The location of the LSDT also receives a large number of cuttings from the bit. Thus, there are excessive cuttings particles accumulated near the LSDT. As shown in Fig. 2, the step surface pushes forward a portion of the cuttings bed as the drill string moves backward axially in the borehole. The solids bed is continuously concentrated in the upper wellbore intervals near the step surface, first forming a cuttings dune, and forming a cuttings cylinder eventually, which is called the “plugging effect of the LSDT”. If a cuttings cylinder is formed, it is only a matter of time before mechanical sticking occurs (Tan and Zhang, 2022). As we all know, larger drilling fluid velocities caused by the large diameter of LSDTs make it easy to clean the cuttings bed in annuli and to transport cuttings particles more quickly. Therefore, the LSDT with a certain tripping velocity may play an unexpected role in the cuttings' removal, which is called the “cleaning effect of the LSDT”.

3. The transient model with multiple flow patterns

3.1. The flow patterns and basic hypotheses

It's well known that the solids bed is inevitable on certain occasions of the horizontal wellbore, such as insufficient displacement, specific drilling operations, inappropriate drilling fluid, etc.

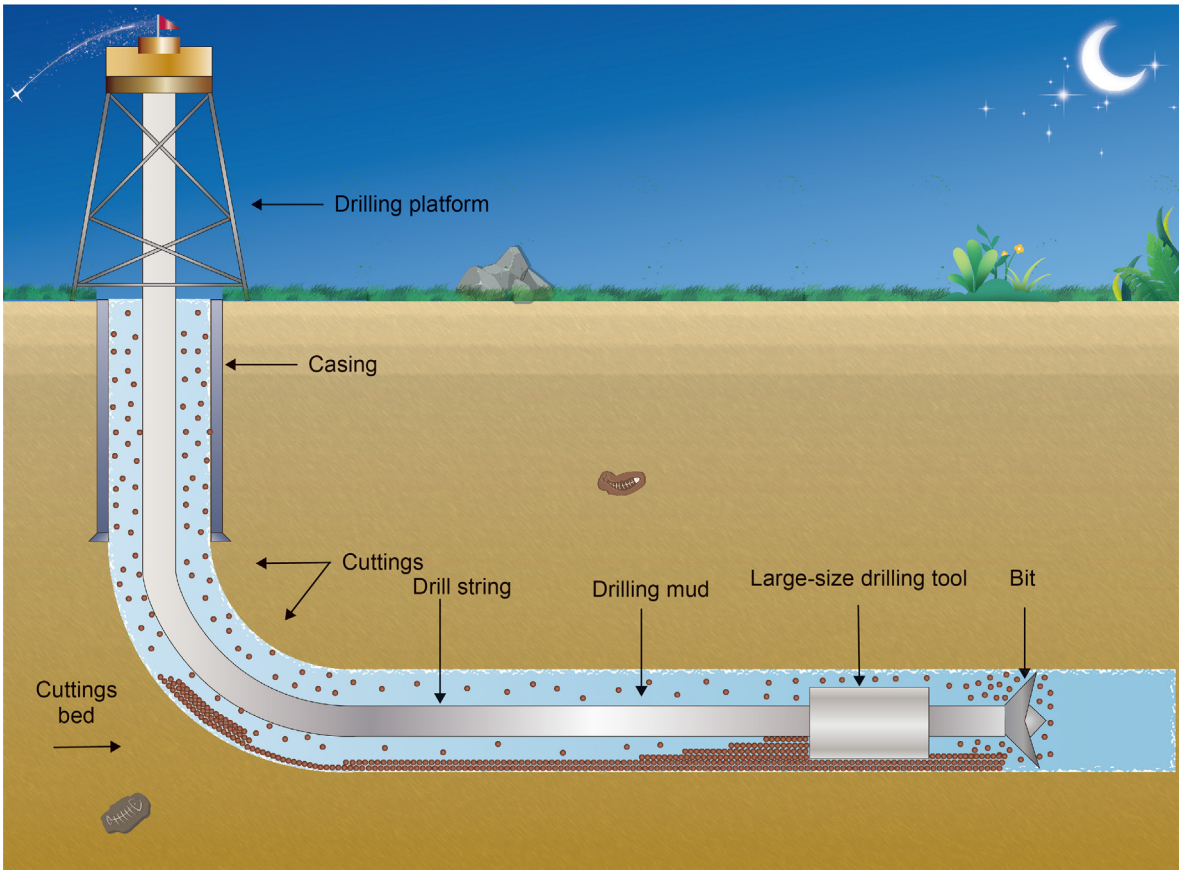

Fig. 1. Backreaming from the bottom hole of the long horizontal section well.

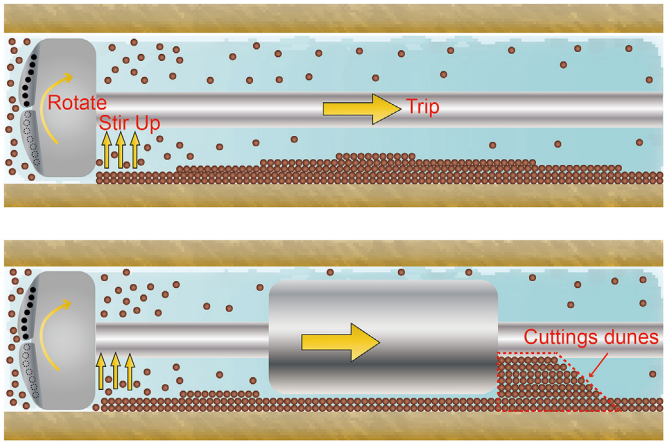

Fig. 2. Backreaming process and bulldozer effect.

Therefore, the coexistence of the suspension layer with cuttings particles and the solid bed layer is a basic flow pattern. But the ultra-high drilling fluid flow rate caused by the LSDTs generally makes the annulus cleaner than other intervals. Considering the flow pattern of fully mixed solid and liquid is indispensable, it indicates that there is only the suspension layer in the annulus. In addition, excessive cuttings bed in upper intervals is formed by the resuspended cuttings transferred from the rotating bit. The annuli with a moving bed or stationary bed are represented by two different flow patterns. Otherwise, the abnormal backflow of the bed would occur in the simulation. In the model, the single-phase flow of liquid with a bed or without a bed is also considered, though the patterns are rare in the main content of this study. The main flow patterns are shown in Fig. 3.

The solids and liquids in the upper suspension layer are considered separately because of slippage between solid particles and liquids (Naganawa et al., 2017; Tong et al., 2021a). This hypothesis is consistent with the phenomenon described by the drift-flux theory (Aitken and Li, 2013). Thus, the solid phase, liquid phase, and bed phase are treated as basic objects in this research. Whether the specific phase exists in a certain flow pattern depends on the conservation of momentum and mass in the annulus. In general, the bit outer diameter is considered equal to the borehole diameter where the enlargement of the borehole diameter is not considered. According to the critical velocity theory, the section through which the bit passes is assumed to be clean because the cross-section is very small and the fluid velocity is large enough. The backreaming operation is a continuous process in engineering practice. In the simulation, the process of backreaming has to be simplified according to the conditions of spatial and temporal discretization, but its engineering characteristics are mostly reflected.

The hypotheses are as follows:

(1) The flow pattern changes according to the flow state;
(2) The solid concentration of the cuttings bed is constant, which is set as 65% (Tong et al., 2021a);
(3) The properties of the fluid and solid are uniform and isothermal in annuli;
(4) Cuttings bed passed by the bit are completely resuspended in the backreaming process;

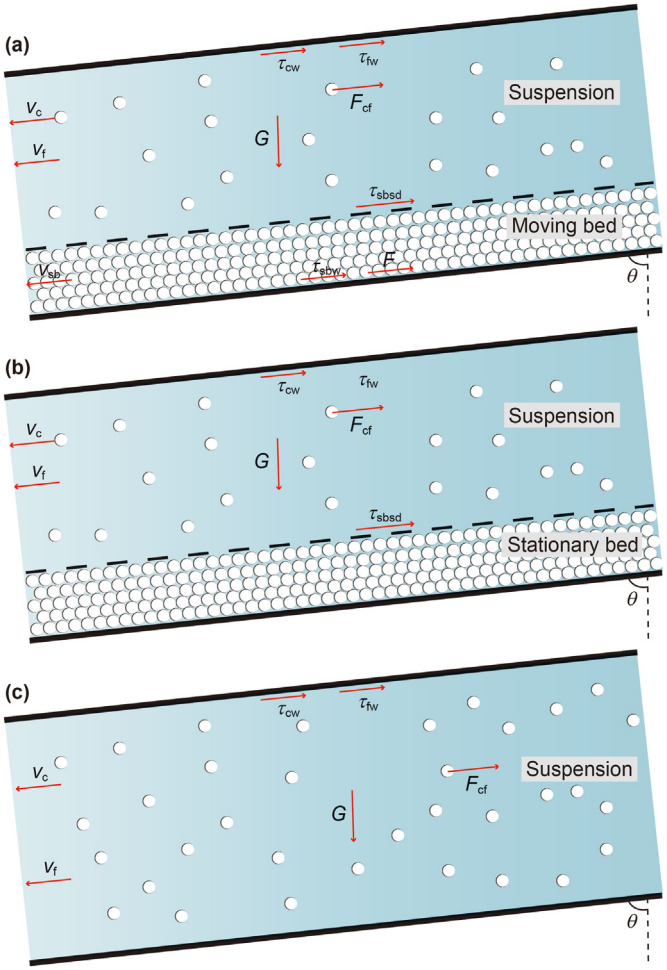

Fig. 3. Main flow patterns in the annuli: (**a**) Moving bed; (**b**) Stationary bed; (**c**) No bed.

(5) There is a slippage between the cuttings and fluid in the suspension layer.
(6) There is no slippage between liquid and particles in the bed layer.

3.2. The modified model

The annulus with the solid-liquid flow in the upper suspension layer and the moving solids bed layer requires the adoption of the most complex flow pattern. The governing equations are constructed according to the law of conservation of mass and momentum for cuttings transport processes.

The mass-conservation equation for the solids bed layer can be expressed as:

$$\frac{\partial(\rho_{sb}A_{sb})}{\partial t}+\frac{\partial(\rho_{sb}A_{sb}v_{sb})}{\partial x}=\Phi_{sb} \tag{1}$$

The mass-conservation equations for solids and liquids in the upper suspension layer are:

$$\frac{\partial(\rho_c C_c A_{sd})}{\partial t}+\frac{\partial(\rho_c C_c A_{sd}v_c)}{\partial x}=\Phi_{sdc} \tag{2}$$

$$\frac{\partial\left(\rho_f C_f A_{sd}\right)}{\partial t}+\frac{\partial\left(\rho_f C_f A_{sd}v_f\right)}{\partial x}=\Phi_{sdf} \tag{3}$$

Fig. 3(a) demonstrates the stress condition of the most complex flow pattern. And the momentum-conservation equation for the bed layer can be expressed as:

$$\begin{aligned}\frac{\partial(\rho_{sb}A_{sb}v_{sb})}{\partial t}+\frac{\partial(\rho_{sb}A_{sb}v_{sb}v_{sb})}{\partial x}=&-A_{sb}\left(\frac{\partial p}{\partial x}+\rho_{sb}g\cos\theta\right)\\&-\tau_{sbw}S_{sb}+\tau_{sbsd}S_{sbsd}-F\\&+v_{sb}\Phi_{sb}\end{aligned} \tag{4}$$

The momentum-conservation equations for liquids and solids in the upper suspension layer are:

$$\begin{aligned}\frac{\partial\left(\rho_f A_{sd}C_f v_f\right)}{\partial t}+\frac{\partial\left(\rho_f A_{sd}C_f v_f v_f\right)}{\partial x}=&-A_{sd}C_f\left(\frac{\partial p}{\partial x}+\rho_f g\cos\theta\right)\\&-C_f\tau_{fw}S_{sd}-C_f\tau_{sbsd}S_{sdsb}-F_{cf}\\&-\left(v_f-v_{sb}\right)\Phi_{sdf}\end{aligned} \tag{5}$$

$$\begin{aligned}\frac{\partial(\rho_c A_{sd}C_c v_c)}{\partial t}+\frac{\partial(\rho_c A_{sd}C_c v_c v_c)}{\partial x}=&-A_{sd}C_c\left(\frac{\partial p}{\partial x}+\rho_c g\cos\theta\right)\\&-C_c\tau_{cw}S_{sd}-C_c\tau_{sbsd}S_{sbsd}+F_{cf}\\&-(v_c-v_{sb})\Phi_{sdc}\end{aligned} \tag{6}$$

The other flow patterns can be simplified based on the most complex one shown above. For the stationary bed, as shown in Fig. 3(b), the velocity of the bed is equal to zero. The mass-conservation equation of the upper suspension layer can be represented by Eq. (2) and Eq. (3) unchangeably. The momentum conservation of the upper suspension layer is written as Eq. (5) and Eq. (6). The mass-conversation of the stationary bed layer can be represented by Eq. (7).

$$\frac{\partial(\rho_{sb}A_{sb})}{\partial t}=\Phi_{sb} \tag{7}$$

For the pattern with no bed, as shown in Fig. 3(c), the mass conversation is shown as:

$$\frac{\partial(\rho_c C_c A_{sd})}{\partial t}+\frac{\partial(\rho_c C_c A_{sd}v_c)}{\partial x}=0 \tag{8}$$

$$\frac{\partial\left(\rho_f C_f A_{sd}\right)}{\partial t}+\frac{\partial\left(\rho_f C_f A_{sd}v_f\right)}{\partial x}=0 \tag{9}$$

$$A_{sd}=A_{ann} \tag{10}$$

The equations of momentum conversation remove some of the quantities associated with the cuttings bed. And the momentum-conservation equations for the solid and the liquid are:

$$\begin{aligned}\frac{\partial\left(\rho_f A_{sd}C_f v_f\right)}{\partial t}+\frac{\partial\left(\rho_f A_{sd}C_f v_f v_f\right)}{\partial x}=&-A_{sd}C_f\left(\frac{\partial p}{\partial x}+\rho_f g\cos\theta\right)\\&-C_f\tau_{fw}S_{sd}-F_{cf}\end{aligned} \tag{11}$$

$$\frac{\partial(\rho_c A_{sd} C_c v_c)}{\partial t} + \frac{\partial(\rho_c A_{sd} C_c v_c v_c)}{\partial x} = -A_{sd} C_c \left(\frac{\partial p}{\partial x} + \rho_c g \cos\theta\right) - C_c \tau_{cw} S_{sd} + F_{cf} \quad (12)$$

The equations of the single-phase flow of liquid with a bed or without a bed are simplified in the same way as above. The conversion process of five flow patterns is shown in Fig. 4.

There is an axial movement of the drill pipe in the backreaming operation. The relative velocities are applied to calculate three kinds of shear stress between the phases and the wall surface. The relative velocity refers to the difference between the phase velocity and the tripping velocity.

Until now three solutions have been employed to obtain the mass exchange fluxes ($\Phi_{sb}, \Phi_{sdf}, \Phi_{sdc}$) between the suspension layer and the bed layer in the previous study, which quantify the cuttings deposition and entrainment. Firstly, an empirical equation method is wildly applied (Naganawa and Nomura, 2006; Naganawa et al., 2017; Zhang et al., 2018; Tong et al., 2021a), in which the mass flux is linearly related to the critical velocity. Secondly, the diffusion mechanism is introduced to quantify the mass flux in the transient cuttings transport model (Zhu et al., 2021, 2022). Thirdly, the mass exchange has two processes according to critical velocity (Chen et al., 2022), which can address some of the shortcomings of the above two approaches. In this model, the third method is applied, of which detail equations are given by Chen et al. (2022), and mass exchange fluxes are given by Tong et al. (2021a). The critical rolling velocity is solved by the near-bed velocity profile not mean velocity (Duan et al., 2009; Tong et al., 2021b), which is useful for the accuracy of the mass exchange flux. Other closure relationships and constructive equations are shown in Appendix A.

3.3. Boundary conditions

3.3.1. Bottom hole

In the backreaming operation, the drilling fluid is squirted out of the bit's water holes and no cuttings are produced in the bottom hole. In other words, the boundary conditions in the bottom hole of the backreaming are the same as those of the condition of washing. Detailed settings are shown in Table 1. With the dynamic mesh method adopted, the position of the bottom hole boundary changes as the bit is pulled out, as shown in Fig. 5. The inner diameter of the pipe of each mesh also changes over calculational time because of the movement of LSDTs.

3.3.2. The mesh adjacent to the bottom hole

One of the important features of the backreaming operation is cleaning the cuttings bed with a rotating bit. In this model, the mesh adjacent to the bottom hole is chosen to simulate the cleaning of the cuttings bed passed by the bit, as shown in Fig. 6. So, the mesh is called the "clean boundary", although it is not a boundary in the traditional sense. The number of cuttings resuspended depends on the values of the tripping velocity, the time step, and the space step. The distance of the backreaming for each time step is calculated by Eq. (13). If the backreaming distance is less than the length of a mesh, the cuttings bed in the mesh is resuspended as cuttings particles in proportion. As shown in Eq. (14), the volume of cuttings particles resuspended at each time step depends on the ratio of the length of the mesh to the distance of the backreaming. The latest bed height and volume concentration of suspended cuttings can be obtained easily according to ΔV_c. When the sum of the backreaming distances reaches the length of a mesh, the cuttings bed in the mesh all become suspended cuttings. The position of the boundary of the bottom hole changes as well. The detailed calculation process is shown in Fig. 6.

$$L_{br} = v_{br} \Delta t \quad (13)$$

$$\Delta V_c = \frac{L_{br}}{\Delta x} A_{sb} \Delta x C_{sb} \quad (14)$$

where v_{br} represents the tripping velocity; Δt represents the time step; Δx represents the spatial step; C_{sb} represents the solid concentration of the solid bed layer.

3.3.3. The meshes associated with the bulldozer effect

As shown in Fig. 7, the cuttings bed of the mesh adjacent to the LSDT which is called "supply mesh" is pushed by the step surface into the next mesh. The cuttings bed height in the "supply mesh" is constant when the LSDT passes through, as shown in Fig. 8. The cuttings bed pushed forward only enters the adjacent mesh which is called "reception mesh", but there is no effect on other meshes. This principle will serve as the basic assumption for quantifying the bulldozer effect. The volume of cuttings bed migration V_{mb} caused by the bulldozer effect can be calculated by Eq. (15).

$$\begin{aligned} A_{sb}(i, t-1) &= \mathrm{HtoA}(d_o, d_i, e, h_c(i)) \\ A_{sb}(i, t) &= \mathrm{HtoA}(d_o, d_{ldst}, e, h_c(i)) \\ V_{mb} &= [A_{sb}(i, t-1) - A_{sb}(i, t)] L_{br} \end{aligned} \quad (15)$$

where A_{sb} represents the cross-sectional area of the cuttings bed; t represents the time step; i represents the index of "supply mesh"; L_{br} is defined as Eq. (13). Due to the bulldozer effect, the cross-sectional area of the cuttings bed in the mesh cell (supply mesh) through which the LSDT passes changes, while the height of the cuttings bed in the mesh cell does not change, as shown in Fig. 8. HtoA is the function in which the cross-sectional area is converted into the cuttings bed height according to the annulus geometry, of which details is given by Zhu et al. (2021).

The cuttings bed from the "supply mesh" are spread evenly in the "reception mesh". The current height of the cuttings bed is calculated by Eq. (16). Through some trial calculations, $\Delta x/\Delta t \geq 4$ should be a criterion for this model of the backreaming simulation, under which the $\Delta x/\Delta t$ has little effect on results and the abnormal termination of iteration does not appear. Therefore, $\Delta x/\Delta t = 4$ is selected in this study.

$$\begin{aligned} A_{sb}(i+1, t-1) &= \mathrm{HtoA}(d_o, d_i, e, h_c(i+1)) \\ A_{sb}(i+1, t) &= A_{sb}(i+1, t-1) + \frac{V_{mb}}{\Delta x} \\ h_c(i+1) &= \mathrm{AtoH}(d_o, d_i, e, A_{sb}(i+1, t)) \end{aligned} \quad (16)$$

where $i+1$ represents the index of "reception mesh". AtoH is the function in which the cuttings bed height is converted into the cross-sectional area according to the annulus geometry.

3.4. Consideration of drill-pipe rotation

As is recognized, the rotation of the drill pipe generally enhances the ability of the drilling fluid to convey cuttings particles and agitate cuttings bed near the lower side of the borehole. However, the mechanism of the effect of drill-string rotation on cuttings transport is quite complex. There is no perfect model to describe the process of cuttings agitated by the revolving drill string for the one-dimensional transient model. In this paper, a preliminary method (Naganawa et al., 2017) is employed to simplify the effect of drill-pipe rotation, in which the fluid velocity of the suspension layer is modified by the linear velocity of the rotational drill pipe, which can be expressed as Eq. (17).

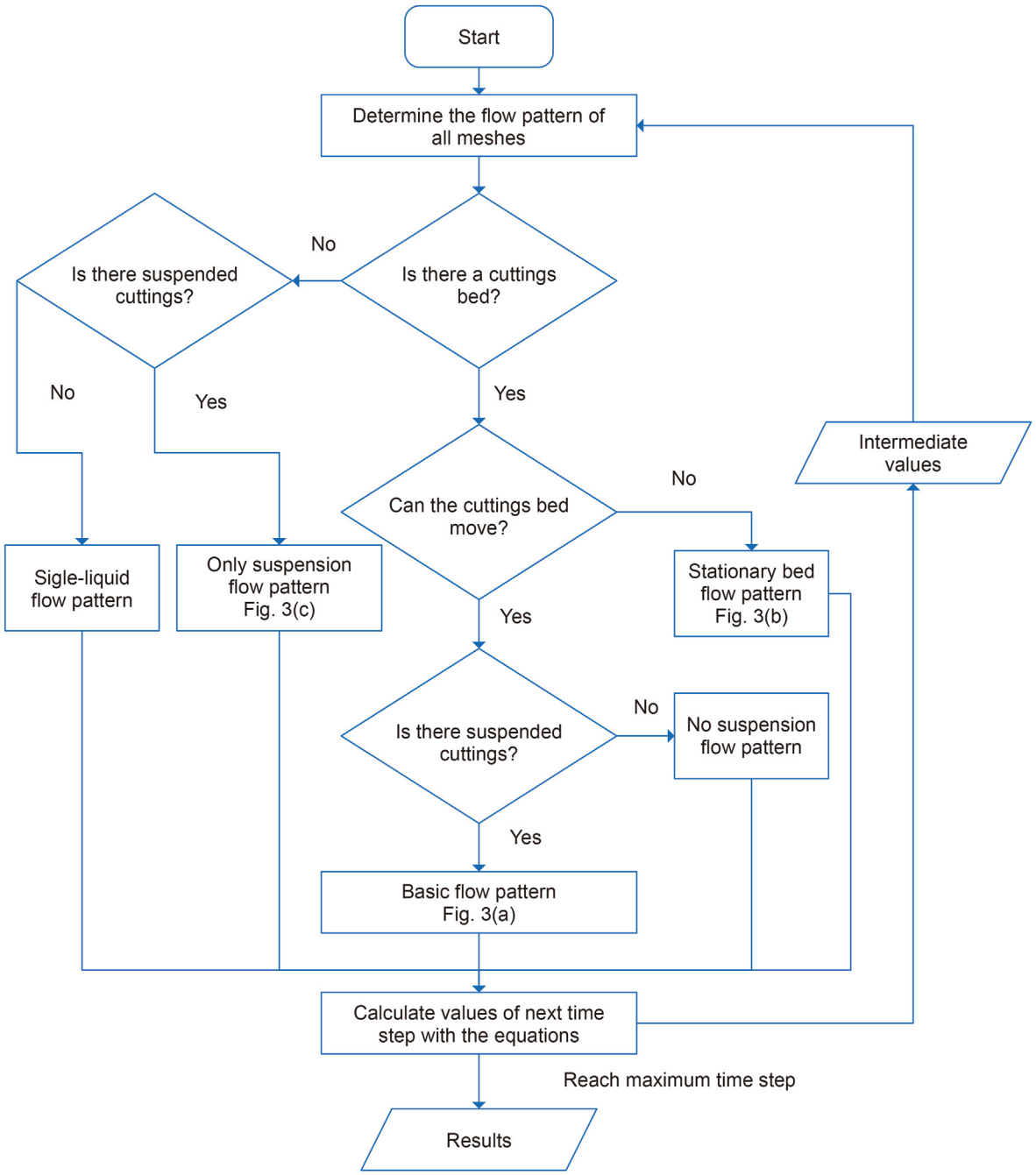

Fig. 4. The conversion of five flow patterns.

$$v_{fr} = \sqrt{{v_f}^2 + {v_a}^2} \tag{17}$$

where the angular velocity at the drill pipe is defined as:

$$v_a = \frac{1}{2}\left(\frac{d_i}{2}\right)\omega_n \tag{18}$$

where the ω_n is the angular velocity of the rotating drill pipe.

In this study, the modified fluid velocity v_{fr} affect mass flux and shear stress (τ_{fw} and τ_{sbsd}). This simplified model describes the effect of drill-string rotation in the case of ensuring computational stability. However, the simulation of drill-string rotation by a one-dimensional model is imperfect compared to a three-dimensional numerical simulation. So, the drill-string rotation speed is not the

Table 1
Boundary conditions of the bottom hole.

Momentum	Mass
$v_f = \frac{4Q_f}{\pi({d_o}^2 - {d_i}^2)(1 - C_c)}$	$C_c = 0$
$v_c = 0$	$A_{sb} = 0$
$v_{sb} = 0$	

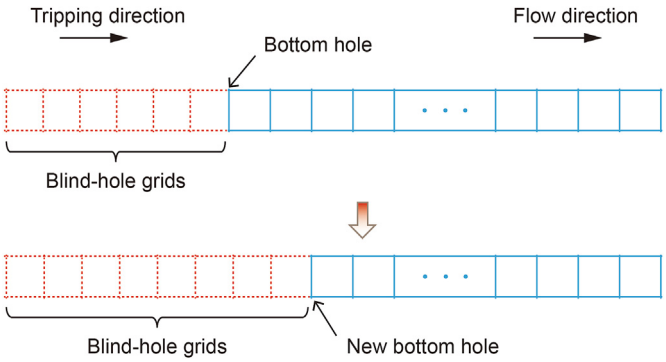

Fig. 5. Dynamic boundary.

focus of the research. The effect of the axial movement of the bit and the LSDT on cuttings transport plays a significant role in the following discussion.

3.5. Numerical solution and mesh setup

In this study, we choose the stability-enhancing two-step (SETS) method to solve the nonlinear differential equations of the transient cuttings transport model (Wang and Long, 2010; Zhu et al., 2021; Chen et al., 2022). The adopted equations in a mesh depend on the corresponding flow pattern, as shown in Section 3.2 of this paper. The method of SETS is developed from the semi-implicit method in which the corrector steps are employed to guarantee precision (Mahaffy et al., 1982). This method removes the

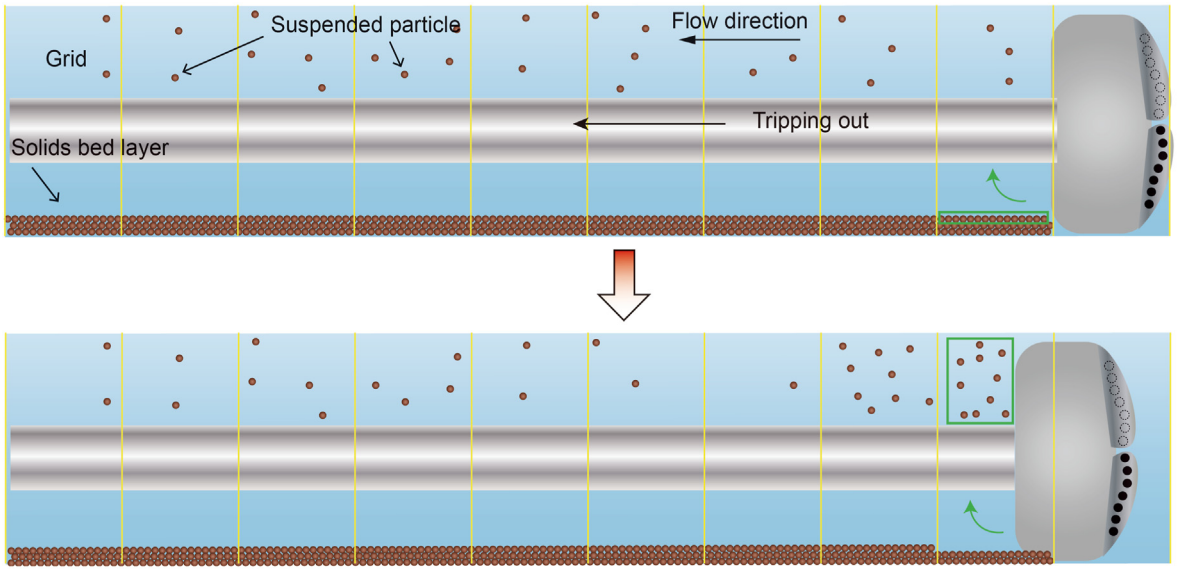

Fig. 6. Resuspended particles near the bit.

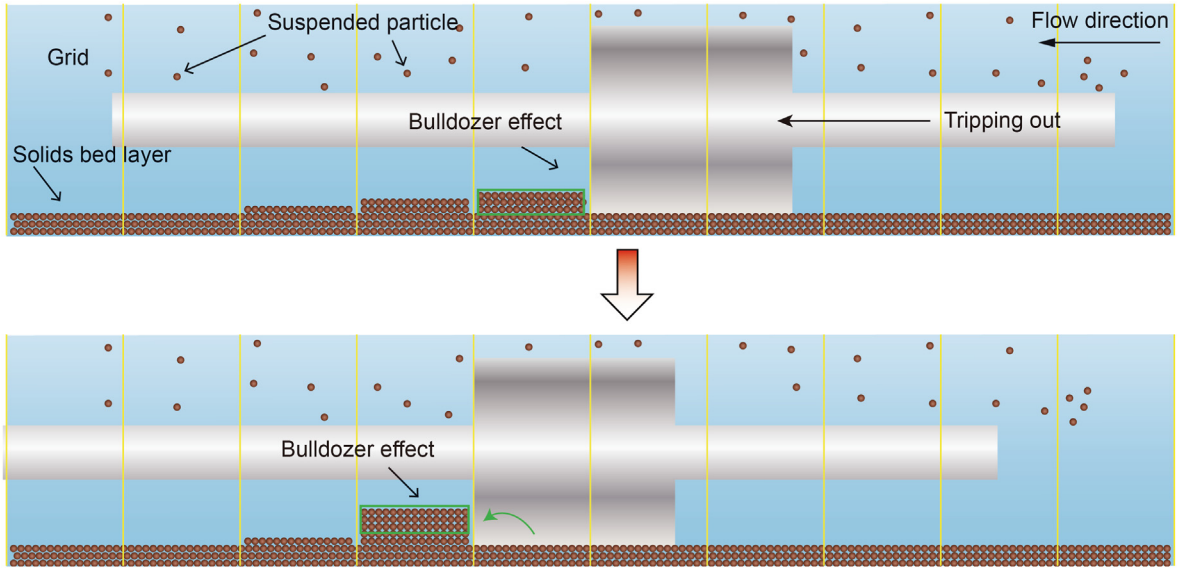

Fig. 7. The front view of the bulldozer effect.

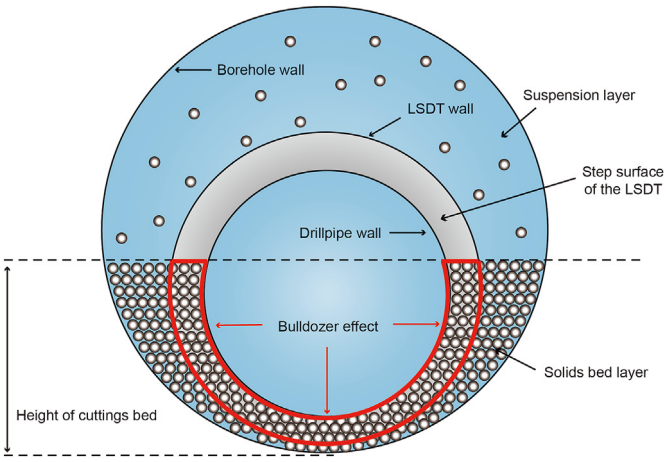

Fig. 8. The slide view of the bulldozer effect.

constraint of the Courant-Friedrichs-Lewy condition in common semi-implicit methods to a certain extent while remains the stability of the computation, which is one of the most important advantages of the SETS method (Naganawa et al., 2017). In other words, more flexible step-size settings enable a reduction of the time required to solve the nonlinear differential equations by the SETS method.

To optimize the mesh step size of the simulation, the mesh independence analysis is carried out for an accurate solution. The simulations of bed erosion are implemented with a 600 m wellbore. It can be found from Fig. 9 that the average cuttings bed height tends to stabilize with the decrease of mesh spacing or the increase of mesh number. When the mesh size is less than 8 m, the mesh size has little effect on the results. The accuracy of calculated results and the efficiency of calculation should be both satisfied as much as possible. Therefore, the mesh size of 4 m is applied for the simulations of cases in this study.

3.6. Verification for the model

The observed data obtained from the large-scale flow-loop system at the University of Tulsa is introduced to verify the basic model (Tong et al., 2021a).

The test section is a 10 m annulus, in which the cuttings bed height is measured through a data acquisition system. The end of the test section can be lifted to change the inclination angle by a hoisting facility. A cuttings injection facility, a mud circulation system, and a cuttings collection facility are employed to simulate the transport of cuttings in the wellbore under drilling conditions. The cuttings bed is deposited evenly and the bed height is set to 50% before the experiments. In the experiment, under a steady flow rate of mud and solid particles, the cuttings bed in the test section is flushed to simulate the process of bed erosion in the drilling operation. Other details can be found in Tong et al. (2021a).

The fluid used in the experiment is an oil-based mud for genuine drilling operations. The flow curve of the mud based on the data measured by a rheometer is given by Tong et al. (2021a) and Herschel-Buckley of the rheological model expressed as $\tau = \tau_y + K\gamma^n$ can describe the fluid properties more comprehensively than the pow-law model. The rheological properties are summarized in Table 2 based on the regression of experimental data, which are applied to subsequent simulations. Therefore, a generalized Reynolds number for Herschel-Buckley is employed, as shown in Appendix A.

The experimental configurations are shown in Table 3. The predations of bed height calculated by the model are in good agreement with the experimental observations, and the error rate is less than ±5%, as shown in Figs. 10 and 11.

4. Results

In this simulation, the properties of fluid and cuttings are consistent with the experimental parameters, but the hole size, drill-pipe size, and fluid flow rate adopted are following the parameters of drilling practice. Default input parameters for all cases are shown in Table 4. Herschel-Buckley of the rheological model is applied in the simulations.

The parameters of backreaming operations and the LSDT lead to the complex law of the cuttings transport, which are the focus of our discussion, and sensitivity analyses are necessary. The main simulated factors include fluid flow rate, tripping velocity, and the diameter and length of the LSDT. However, the initial cuttings bed in the wellbore has an important influence on the simulation results, although it is artificially set. Therefore, it is necessary to explain the effect of the initial cuttings bed height first to avoid confusion in the analyses of the main factors.

4.1. Case 1: effect of the initial cuttings bed

The input parameters are shown in Table 5. The influence of initial cuttings bed height on cuttings transport is phased and nonlinear, as shown in Fig. 12. The reason for this phenomenon is that the amount of cuttings bed driven by the step surface is not uniform in an eccentric annulus, as shown in Fig. 8. There is a critical value for the initial cuttings bed height, and the bulldozer effect on both sides presents completely different laws. When the initial cuttings bed height is greater than the critical value, the cuttings accumulate excessively in the intervals behind the step surface, as shown in Fig. 12(a), (b), and (c). Moreover, as the height of the initial cuttings bed increases, the accumulation range and peak value of the cuttings bed increase, which indicates that these two variables require additional attention in this study. When the initial height of the cuttings bed is less than the critical value, the backreaming operation improves the wellbore cleaning efficiency, as shown in Fig. 12(d). To explore the stuck pipe mechanism in the backreaming operation, 30% of the initial dimensionless cuttings bed height is employed in subsequent simulations. The case that the initial cuttings bed height is below the critical value is not the focus of our discussion.

4.2. Effect of the LSDT

It can be found that the bulldozer effect in the backreaming operation has a significant impact on the calculation results from the above analyses. Therefore, it is necessary to analyze the mechanism of the LSDT on cuttings redistribution. We will discuss the role of operation parameters later.

4.2.1. Case 2: effect of the diameter

The parameters for Case 2 are shown in Table 6. At the beginning of the backreaming, the cuttings bed accumulated in the wellbore does not decrease rapidly due to washing, because the bit continually destroys the cuttings bed and transports cuttings particles to the upper sections, as shown in Fig. 13(a). As long as there are LSDTs, there would be a large number of cuttings in front of the step surface, which indicates that the intervals with higher cuttings bed appear, as shown in Fig. 13(b), (c), (d). A section with cuttings bed height greater than the initial height can be defined as a hazardous section and its length is represented by L_{haz}. The length of the

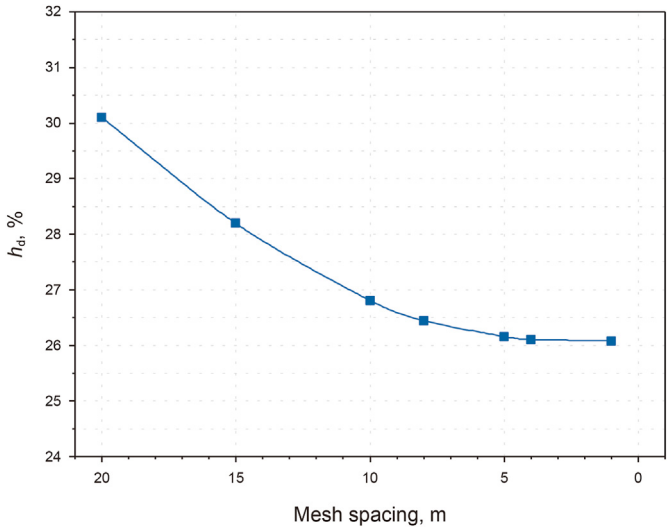

Fig. 9. Mesh independence study for the model.

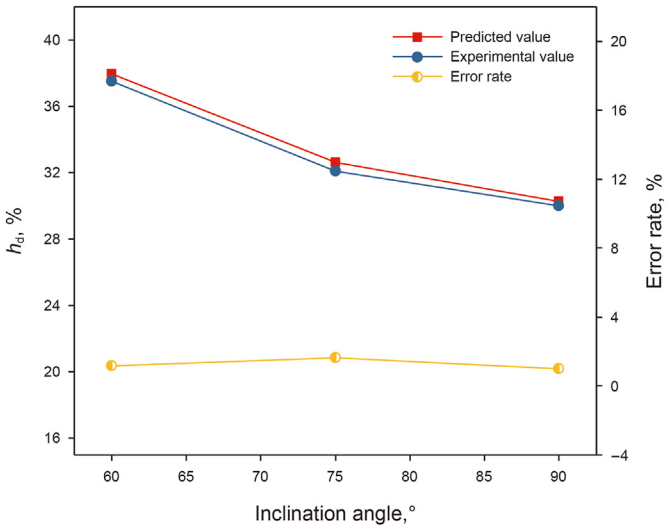

Fig. 11. Steady cuttings bed at 30 m/h of ROP.

Table 2
Rheological properties.

Variables	Value	Unit
Consistency coefficient	0.02	Pa•s^n
Liquidity index	0.9	Dimensionless
Yield strength	0.12	Pa
Density of fluid	1200	kg/m^3

Table 3
Experimental parameters.

Variables	Value	Unit
Fluid flow rate	0.0025	m^3/s
ROP	15, 30	m/hour
Particle diameter	0.003	m
Inclination angle	60, 75, 90	°
Density of cuttings	2630	kg/m^3
Outer pipe diameter	0.0762	m
Inner pipe diameter	0.0381	m
Eccentricity	0.7	Dimensionless

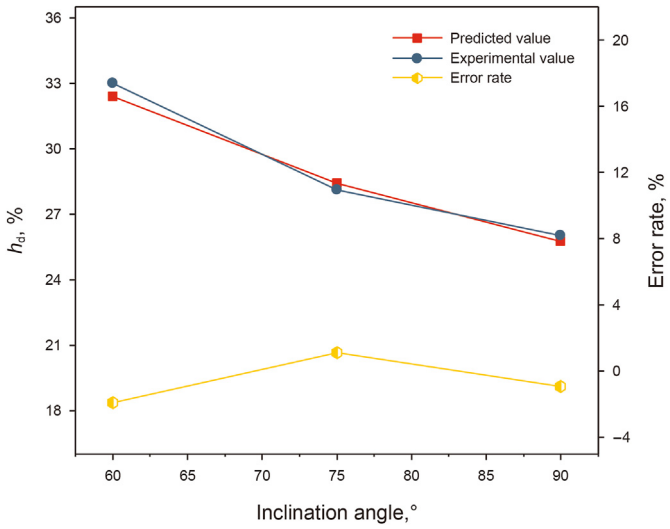

Fig. 10. Steady cuttings bed at 15 m/h of ROP.

Table 4
Default parameters for the model.

Variables	Value	Unit
Consistency coefficient	0.02	Pa•s^n
Liquidity index	0.9	Dimensionless
Yield strength	0.12	Pa
Density of fluid	1200	kg/m^3
Density of cuttings	2630	kg/m^3
Eccentricity	0.4	Dimensionless
Particle diameter	0.003	m
Inclination angle	90	°
Pipe length between LSDT and bit	8	m
Outer pipe diameter	0.2159	m
Inner pipe diameter	0.127	m
Drill-pipe rotation speed	30	r/min

Table 5
Input parameters for Case 1.

Variables	Value	Unit
Initial cuttings bed height	30, 20, 10, 5	%
Fluid flow rate	35	L/s
LSDT diameter	0.1788	m
LSDT length	4	m
Tripping velocity	0.5	m/s

hazardous sections remained largely stable at diameters of 0.1588 and 0.1651 m of LSDTs, as shown in Fig. 14. To show the trend of the results more clearly, darker lines are introduced which represent the average of the data in the figures. The average method is to take the average of seven data around the target data, which is very common in the processing of time-varying data, such as oscilloscope data. When the diameter is 0.1788 m, the length of the hazardous section increases as the backreaming distance increases. As shown in Fig. 14, the change of the hazardous length at diameters of 0.1588 and 0.1651 m of LSDTs can be divided into three stages: increase, maintain, and decrease. And the length of the hazardous section at diameters of 0.1788 m increases first and then stabilizes. The larger the size of the LSDT, the longer the hazardous section and the easier it is to maintain while backreaming.

Since the vicinity of the LSDT is the key area causing mechanical sticking, the $h_{d,aver}$ is introduced, which represents the average of dimensionless cuttings bed height of the section from 0 to 20 m

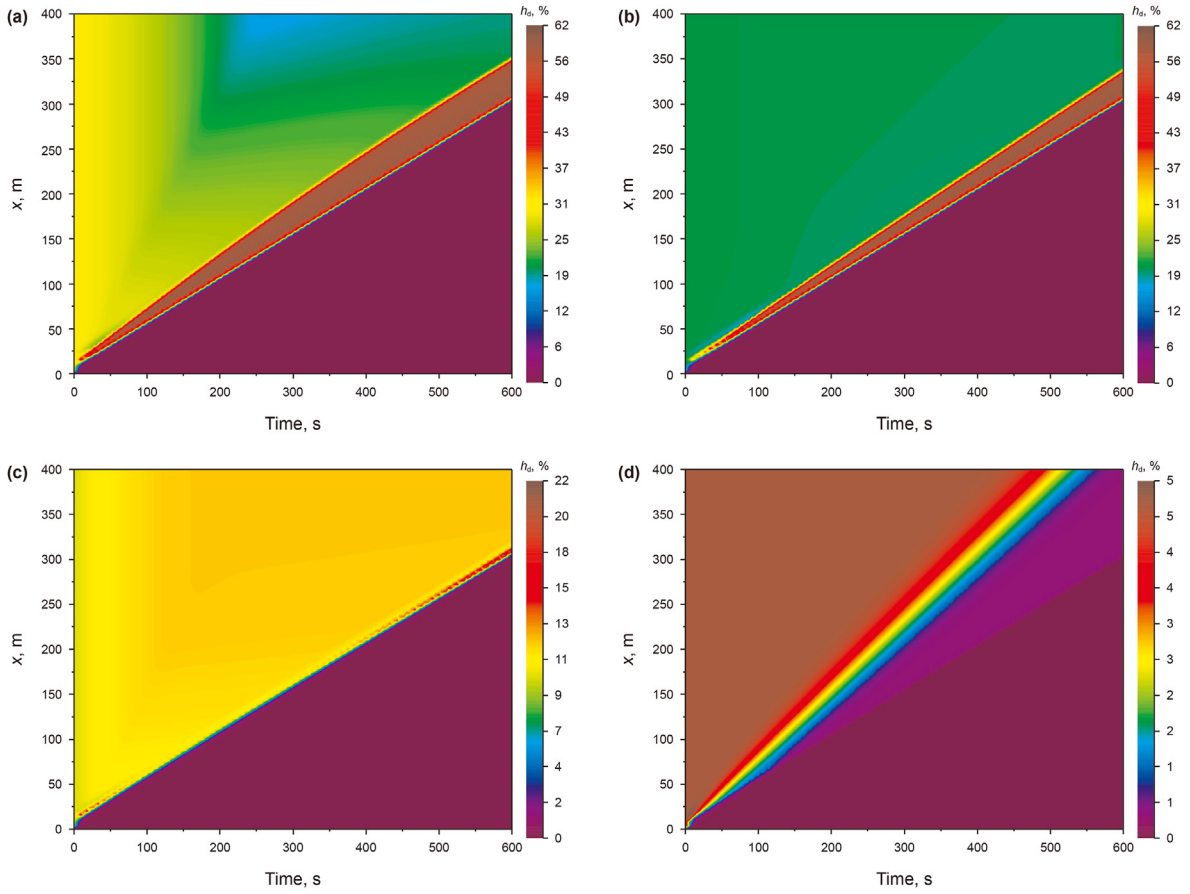

Fig. 12. Simulation results of different initial dimensionless heights of cuttings bed: (**a**) 30%; (**b**) 20%; (**c**) 10%; (**d**) 5%.

Table 6
Input parameters for Case 2.

Variables	Value	Unit
LSDT diameter	0.1788, 0.1651, 0.1588, 0.1270	m
Fluid flow rate	35	L/s
Initial cuttings bed height	30	%
LSDT length	4	m
Tripping velocity	0.5	m/s

(and 0–40 m) from the LSDT in annuli. As shown in Fig. 15, when the diameter of the LDST is 0.1788 m, the $h_{d,aver}$ remains stable after 150 s of the backreaming. The $h_{d,aver}$ reaches its maximum after 165 s of the backreaming and then gradually decreases when the diameter of the LSDT is 0.1651 m. The $h_{d,aver}$ reaches its maximum after 90 s of the backreaming and then drops gradually when the diameter of the LSDT is 0.1588 m. By comparing those four curves, it can be found that the larger the LSDT diameter is, the greater the accumulation of cuttings behind the step surface and the longer the high cuttings bed remains.

In addition, to reveal the severity of cuttings accumulation, the $h_{d,max}$ is introduced, which represents the maximum of dimensionless cuttings bed height of the whole wellbore. Due to the $h_{d,max}$ is highly cyclical, only those average value is shown in Fig. 16, which indicate the trend of the maximum of dimensionless cuttings bed height in the whole process. The original $h_{d,max}$ varies between 59% and 62% most of the time when the diameter of the LDST is 0.1788 m. When the diameter of the LDST is 0.1651 m, the $h_{d,max}$ ranges from 51% to 61% most of the time. The $h_{d,max}$ varies between 43% and 55% most of the time when the diameter of the LDST is 0.1588 m.

In a word, the larger the diameter of the LSDT, the longer the hazardous section, the more cuttings bed in front of the step surface, and the larger the peak value of cuttings deposition. There is a critical diameter of the LSDT for cuttings transport while backreaming. If the diameter of the LSDT is larger than the critical value, the "plugging effect of the LSDT" is dominant; otherwise, the "cleaning effect" is dominant. For the bit, at the beginning of the backreaming, the "plugging effect" is much stronger than the "cleaning effect", because the distribution of cuttings bed is more uniform. As the backreaming is continuously performed, the "cleaning effect" of the bit is gradually dominant, due to the concentration of cuttings bed in front of the step surface.

4.2.2. Case 3: effect of the length

The parameters for Case 3 are shown in Table 7. Fig. 17 shows that the accumulation of cuttings near the step surface increases as the length of the LSDT increases. It can be found that there is a certain difference in the lengths of the wellbore interval with significantly higher cuttings bed when the lengths of LSDTs are 4 and 8 m. If the length of the LSDT is larger than 8 m, the characteristics of cuttings accumulation display a slight difference with the increase of the length of the LSDT. However, it is obvious that the length of the wellbore section (far away from the bit) with low cuttings bed height increases as the length of the LSDT increases, which indirectly indicates that cuttings accumulation in the upper section becomes more serious. This phenomenon can be further explained by the length of the hazardous section. As shown in

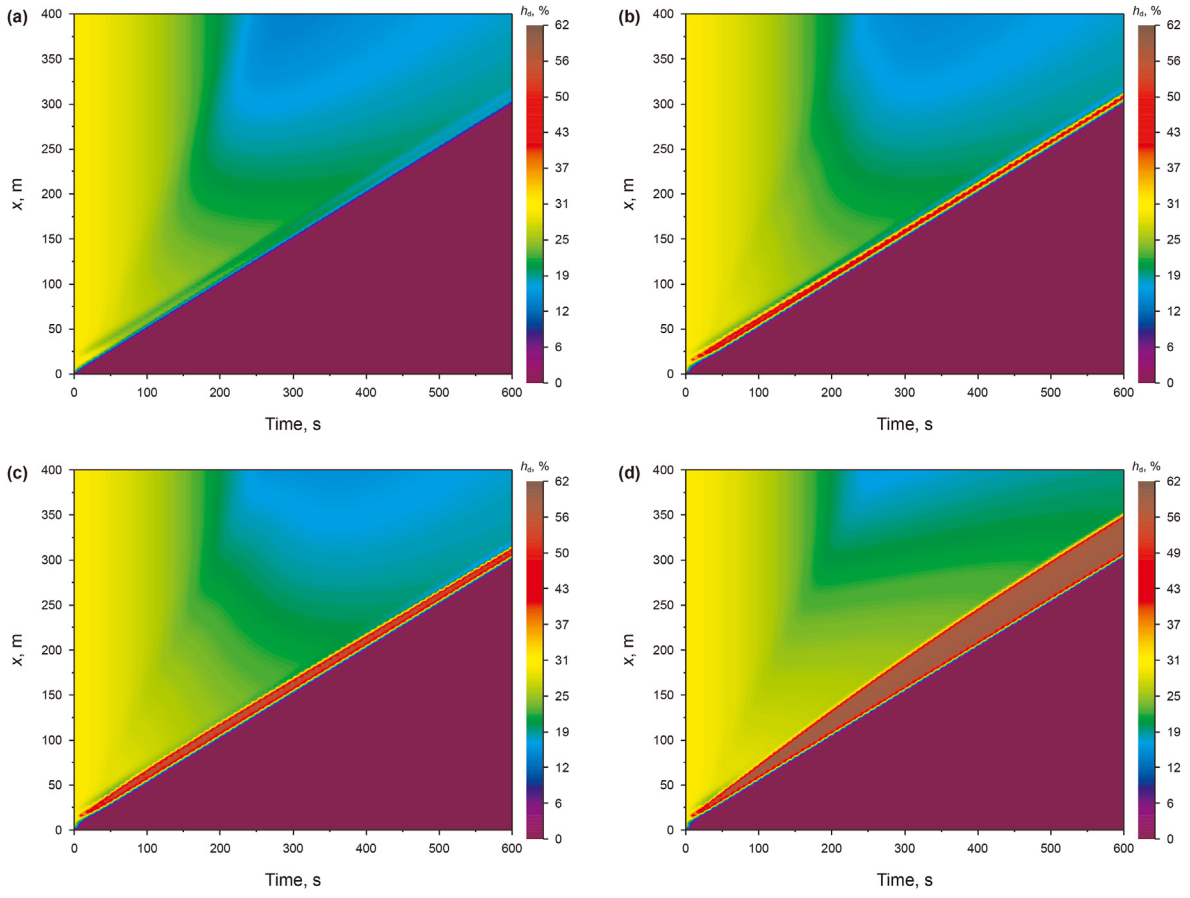

Fig. 13. Simulation results of different diameters of LSDTs: (**a**) 0.1270 m; (**b**) 0.1588 m; (**c**) 0.1651 m; (**d**) 0.1788 m.

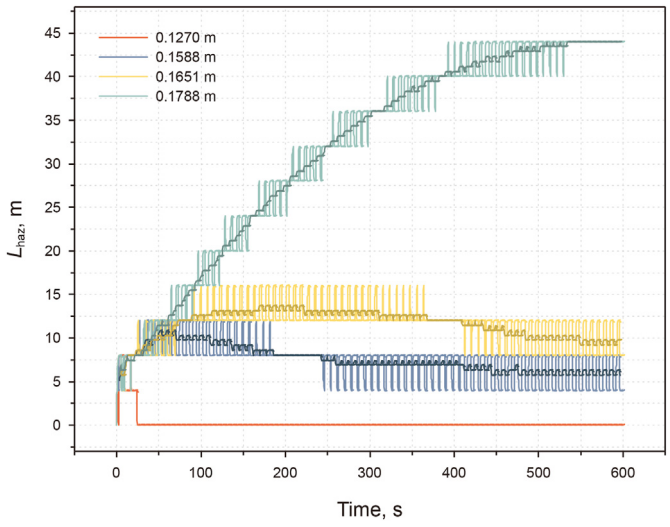

Fig. 14. The lengths of hazardous sections of different diameters of LSDTs.

Fig. 18, when the length of the LSDT is 4 m, the hazardous section is shorter than those in the other three cases. After backreaming of 600 s, the length of the hazardous section at 4 m of the LSDT is about 45% shorter than those in the other three cases. In addition, the length of the hazardous section at 12 m of the LSDT is longer than that at 16 m of the LSDT after backreaming of 400 s, which indicates there is a specific length of the LSDT which could cause more cuttings in the wellbore. According to the calculations so far, 12 m of LSDT is more dangerous than other ones for backreaming operations.

Strictly speaking, the longer the LSDT is, the greater the average height of the cuttings bed in the section near the step surface, as shown in Fig. 19. It is found that the average heights of cuttings bed with different lengths of LSDTs has little difference in general when those reach the stable stage. However, it is very obvious that the longer the LSDT is, the more easily the cuttings deposition near the step surface reaches a stable situation. The calculated results of 40 m above the step surface explain the phenomenon better than those of 20 m above the step surface, as shown in Fig. 19(a) and (b). But when the length of the LSDT is beyond 4 m, the rate of reaching stability is close. There is a similar pattern for the peak of the cuttings bed height, as shown in Fig. 20.

For the hazardous sections, the shorter LSDT could avoid the risk of the stuck pipe in backreaming operations to a great extent. But the lengths of LSDTs show a slight effect on the average height of the cuttings bed near the step surface and the peak value of cuttings deposition when those reach a stable stage.

4.3. Effect of the operation parameters of the backreaming

4.3.1. Case 4: effect of the flow rate

The parameters for Case 4 are shown in Table 8. According to the simulation results, the flow rate is not simply a positive or negative correlation to hole cleaning in backreaming operations. Based on the accumulation characteristics of the cuttings bed, the flow rate can be classified as “dangerous flow rate”, “low flow rate” and “high

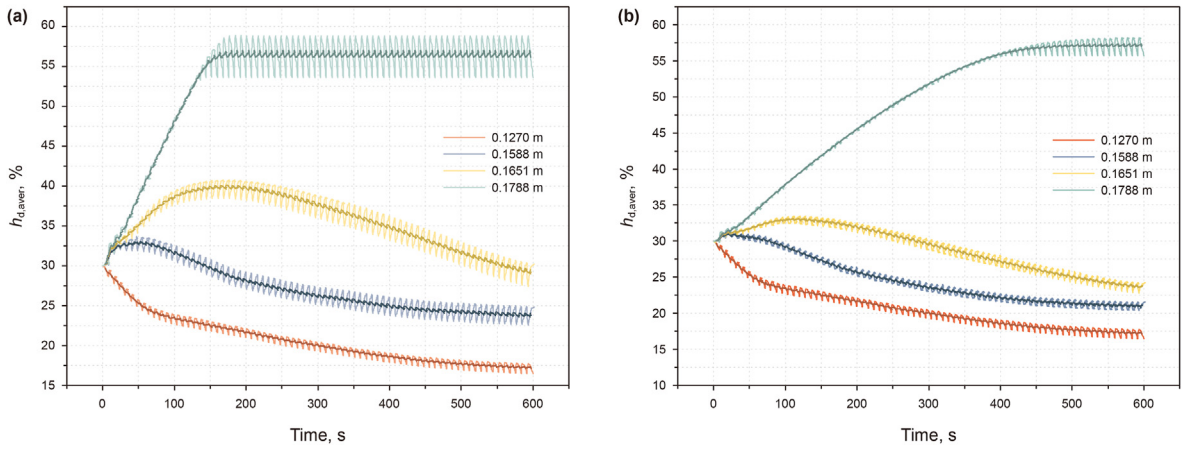

Fig. 15. The average dimensionless cuttings bed heights of different diameters of LSDTs: (**a**) 20 m above the step surface; (**b**) 40 m above the step surface.

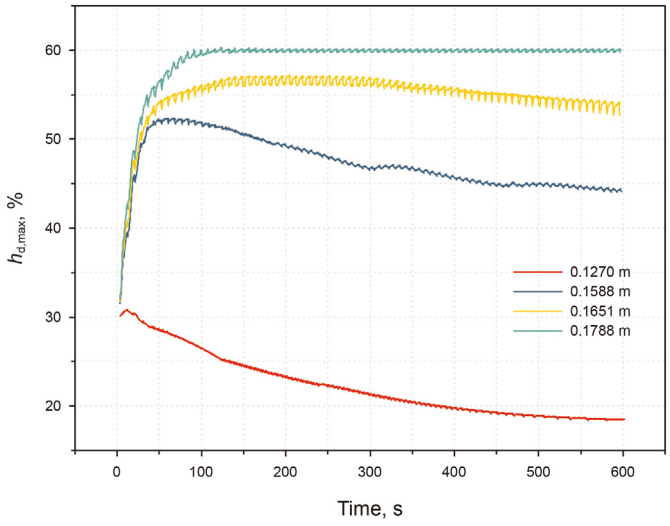

Fig. 16. The maximum dimensionless cuttings bed heights different diameters of LSDTs.

flow rate", separately. Through some calculations, we have found that 32, 32.5, and 32.7 L/s caused a complete blockage of the wellbore during the backreaming in this simulation, in which the stuck pipe is considered inevitable. Therefore, we call the flow rate less than 33 L/s a "dangerous flow rate" in this simulation. The "plugging effect" of the bit dominates in the case of extra-low annular flow velocity, and the "cleaning effect" of the LSDT is not sufficient to transport excessive cuttings, where the bulldozer effect even causes annular jams due to low cuttings migration velocity. The "low flow rate" interval indicates the range in which the flow rate is 33–35 L/s, and the length of the wellbore with excessive cuttings bed near the step surface increases with increasing flow rate, as shown in Fig. 21(a) and (b). The length of the hazardous section and average cuttings bed height are important indicators for this definition. The "plugging effect" of the bit decreases with increasing flow rate, but the "cleaning effect" of the LSDT is relatively weaker because of the increase of cuttings transport velocity.

As the flow rate increases to the "high flow rate" interval (>35 L/s), the length of the wellbore with significantly high cuttings bed near the step surface decreases continuously, as shown in Fig. 21(c) and (d). The length of the hazardous section and average cuttings bed height decreases with the increase of the flow rate. The

Table 7
Input parameters for Case 3.

Variables	Value	Unit
LSDT diameter	0.1788	m
Fluid flow rate	35	L/s
Initial cuttings bed height	30	%
LSDT length	4, 8, 12, 16	M
Tripping velocity	0.5	m/s

distribution of cuttings bed with a flow rate of 42.5 L/s is different from those in the other three cases, where the cuttings bed is more evenly distributed and there is no significant accumulation of cuttings bed, as shown in Fig. 21(e) and (f). It has been calculated that if the flow rate continues to increase, the wellbore becomes cleaner.

As shown in Fig. 22, the length of the hazardous section with the flow rate of 35.0 L/s is 44 m after the backreaming of 600 s. When the fluid flow rates are 37.5, 40, and 42.5 L/s, the lengths of hazardous sections decrease by 15.6%, 49.4%, and 100% respectively compared with that of 35.0 L/s. The smaller the flow rate in the "high flow rate" interval, the greater the length of the hazardous section in the backreaming operation. If the flow rate is more than 40 L/s, the hazardous section only exists in the early period of the backreaming, and then disappears quickly. However, if the flow rate is in the "low flow rate" interval, smaller flow rates have a shorter hazardous section instead.

The average dimensionless cuttings bed height in the 20 m interval above the step surface after the backreaming of 600 s is 46.4%, 56.2%, 54.1%, 50.8%, 5.7%, and 0% respectively at different flow rates, as shown in Fig. 23(a). It can be found that the higher the flow rate in the "high flow rate" interval, the smaller the cuttings bed height near the step surface, but the relationship between those two is nonlinear. In this study, there is a critical flow rate that changes the distribution of cuttings bed in the backreaming process, which is 40 L/s. As the flow rate is less than 40 L/s, the cuttings bed height near the step surface gradually increases and then remains stable with the progress of the backreaming; otherwise, the height continuously decreases to zero. A similar pattern can be seen from the data of 40 m of the interval, as shown in Fig. 23(b). When the flow rate is 33 L/s in the "low flow rate" interval, the area near the step surface is cleaner than that of 35 L/s. It is not the case that the larger the displacement, the better the hole cleaning near the step surface in the backreaming process. Admittedly, it is possible to reduce the buildup of the cuttings bed if the displacement is high

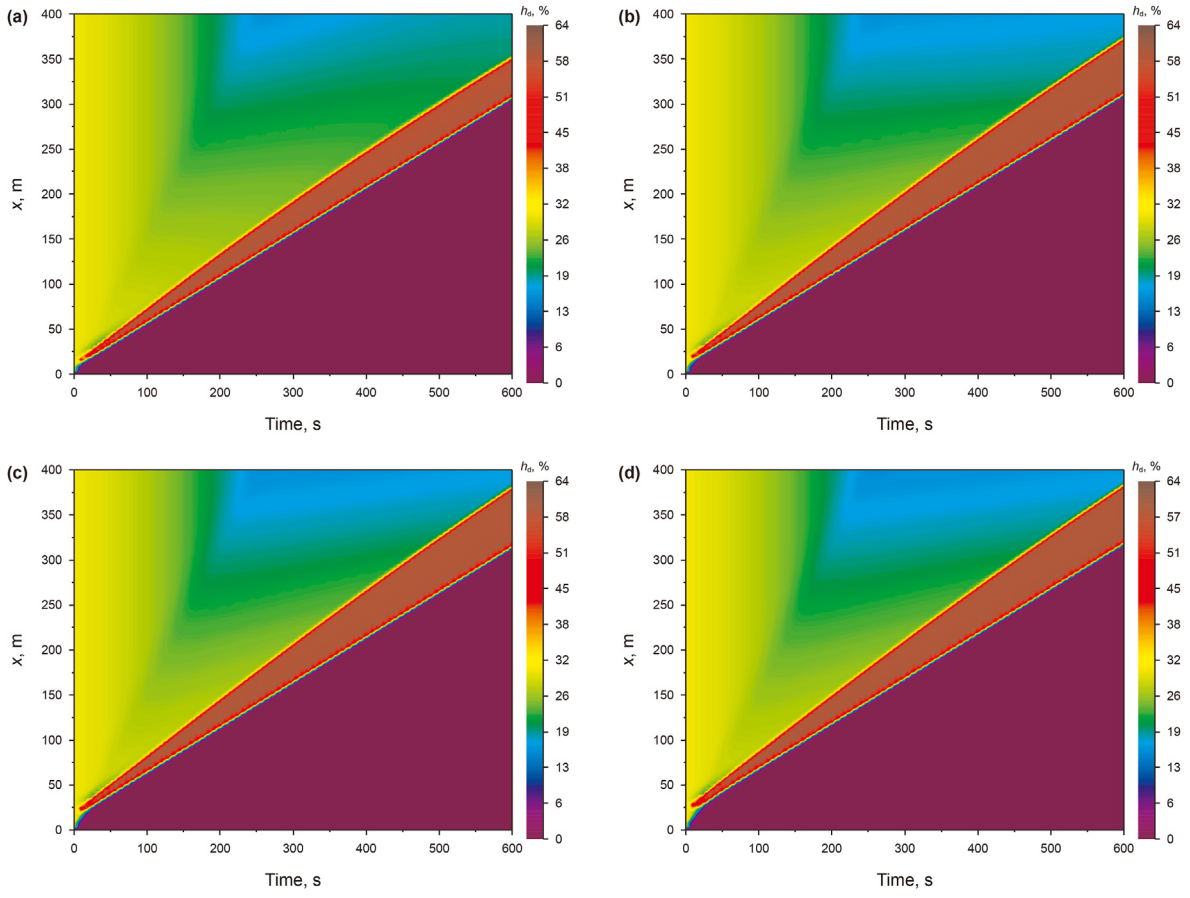

Fig. 17. Simulation results of different lengths of LSDTs: (**a**) 4 m; (**b**) 8 m; (**c**) 12 m; (**d**) 16 m.

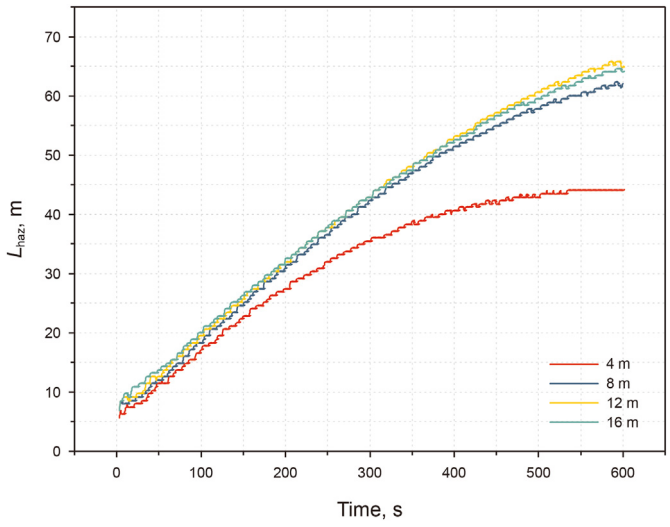

Fig. 18. The lengths of hazardous sections of different lengths of LSDTs.

enough, but this can only be done by finding the "high flow rate" interval needed on site. In addition, for pressure-sensitive formations, adopting a lower displacement in the "low flow rate" interval can both avoid jams during backreaming operations and keep the stability of the good wall.

The peak cuttings bed height in the wellbore decreases with increasing flow rate, as shown in Fig. 24. If the flow rate is more than 40 L/s, the maximum height decreases with time; otherwise, it increases first and then keeps stable. This is consistent with the rule of the length of the hazardous section and the average height of the cuttings bed near the step surface. The peak cuttings bed height in the wellbore with a flow rate of 33 L/s is maximum although the wellbore as a whole is relatively clean, which indicates the flow rate has a significant effect on peak height. Therefore, the low flow rate needs to be employed carefully.

4.3.2. *Case 5: effect of the tripping velocity*

The parameters for Case 4 are shown in Table 9. When the slip velocity is 0.2 m/s, there is no excess cuttings accumulation near the step surface, as shown in Fig. 25(a). The reason is that a large amount of cuttings bed in annuli had been transported to the upper intervals of the wellbore before the LSDT arrived due to low tripping velocity. In this situation, though the LSDT has a slight effect on the distribution of cuttings beds, it still mitigates the influence of the "plugging effect" of the bit. Therefore, the borehole is in clean condition. When the tripping velocity increases to 0.4 m/s, the accumulation of cuttings bed caused by the bulldozer effect appears, and the "plugging effect" is stronger than the "cleaning effect", as shown in Fig. 25(b). When the tripping velocity is 0.5 m/s, the accumulation of cuttings bed near the step surface becomes more serious than that of the tripping velocity of 0.4 m/s, and the "plugging effect" is further enhanced, as shown in Fig. 25(c). When the tripping velocity reaches 1.0 m/s, the total length of the intervals with excessive cuttings beds above the step surface significantly reduces, and the "clean effect" becomes the main function of the LSDT, as shown in Fig. 25(d). Though the cuttings beds coalesce

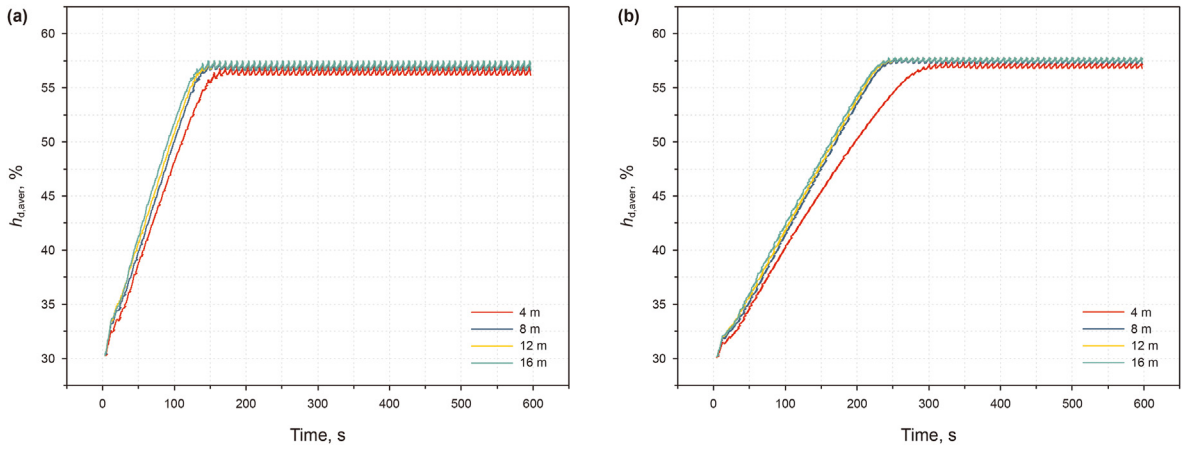

Fig. 19. The average dimensionless cuttings bed heights of different lengths of LSDTs: (**a**) 20 m above the step surface; (**b**) 40 m above the step surface.

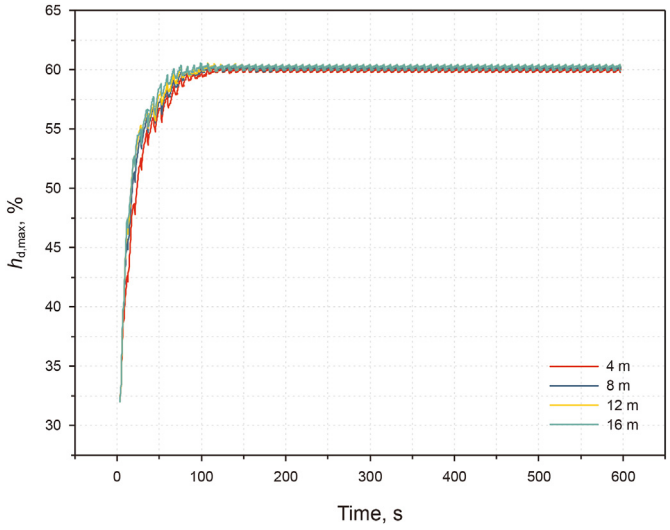

Fig. 20. The maximum dimensionless cuttings bed heights of different lengths of LSDTs.

Table 8
Input parameters for Case 4.

Variables	Value	Unit
LSDT diameter	0.1788	m
Fluid flow rate	33, 35, 37.5, 40.0, 42.5, 45	L/s
Initial cuttings bed height	30	%
LSDT length	4	m
Tripping velocity	0.5	m/s

quickly in front of the step surface, the excessive cuttings bed is immediately dispersed due to the high flow velocity caused by the LSDT. Therefore, temporary accumulation of the cuttings bed under a high tripping velocity increases the efficiency of hole cleaning, and the "cleaning effect" of LSDT is completely dominant. From the perspective of the rule of thumb, if the tripping velocity is too fast, it is easy to cause annular blockage. However, based on simulation results, it can be found that the rule of thumb only works to a certain extent of tripping velocity, of which the interval is 0.4–0.5 m/s in this case. When the tripping velocity increase to 1.0 m/s, the hole cleaning is getting better. Therefore, we define an interval called the "dangerous velocity", in which more cuttings beds are accumulated near the LSDTs obviously than those of other velocities. As long as the tripping velocity is far away from the "dangerous velocity", the stuck accident can be avoided in the backreaming process to the greatest extent. In addition, the tripping velocity should not be too large, because the rapid accumulation of cuttings bed may directly lead to stuck pipe in the initial stage of backslide.

Fig. 26 indicates that the lengths of the hazardous section with tripping velocities of 0.4 and 0.5 m/s are larger than those of other ones, which is consistent with the rules stated above. It is worth noting that the hazardous section with 0.4 m/s is longer than that of one with 0.5 m/s after the backreaming of 300 m because the cuttings distribution is more concentrated when tripping velocity is 0.5 m/s which is supported by Figs. 27 and 28. The higher the tripping velocity, the more concentrated the distribution of cuttings beds when it is in the "dangerous velocity" range. The average dimensionless cuttings bed height in the interval of 20 m above the step surface is 0%, 53.6%, 56.2%, and 22.4% respectively at different tripping velocities after the backreaming of 300 m, as shown in Fig. 27(a). A similar pattern can be seen from the data of 40 m interval, as shown in Fig. 27(b).

5. Discussion

The effects of the annular geometry, particle properties, inclination angle, and drilling fluid properties on the results are discussed to provide a more comprehensive explanation of the cuttings transport mechanism under the backreaming operation. The factor analyses are employed in this section. The average of dimensionless cuttings bed height of the section from 0 to 40 m from the LSDT in annuli $h_{d,aver}$ is used as an indicator of results, which is conducive to the two-factor analyses. The $h_{d,aver}$ mainly reflects the risk of the stuck pipe caused by the accumulation of cuttings near LSDTs.

It is found by calculation results that a more serious deposition of cuttings appears in the section with the smaller inclination angle (<90°). The distance of backreaming can reach 300 m with a 90-degree inclination angle and 37.5 L/s flow rate. For a 75-degree inclination angle, the maximum distance of backreaming only reaches 138 m with the same flow rate. For a 60-degree inclination angle, the maximum distance of backreaming only reaches 100 m. In a word, the inclined section has a higher risk of stuck pipe compared with the horizontal section. In addition, the wellbore section with less than 60° inclination angle is prone to serious avalanche and downward sliding of the cuttings bed which are not

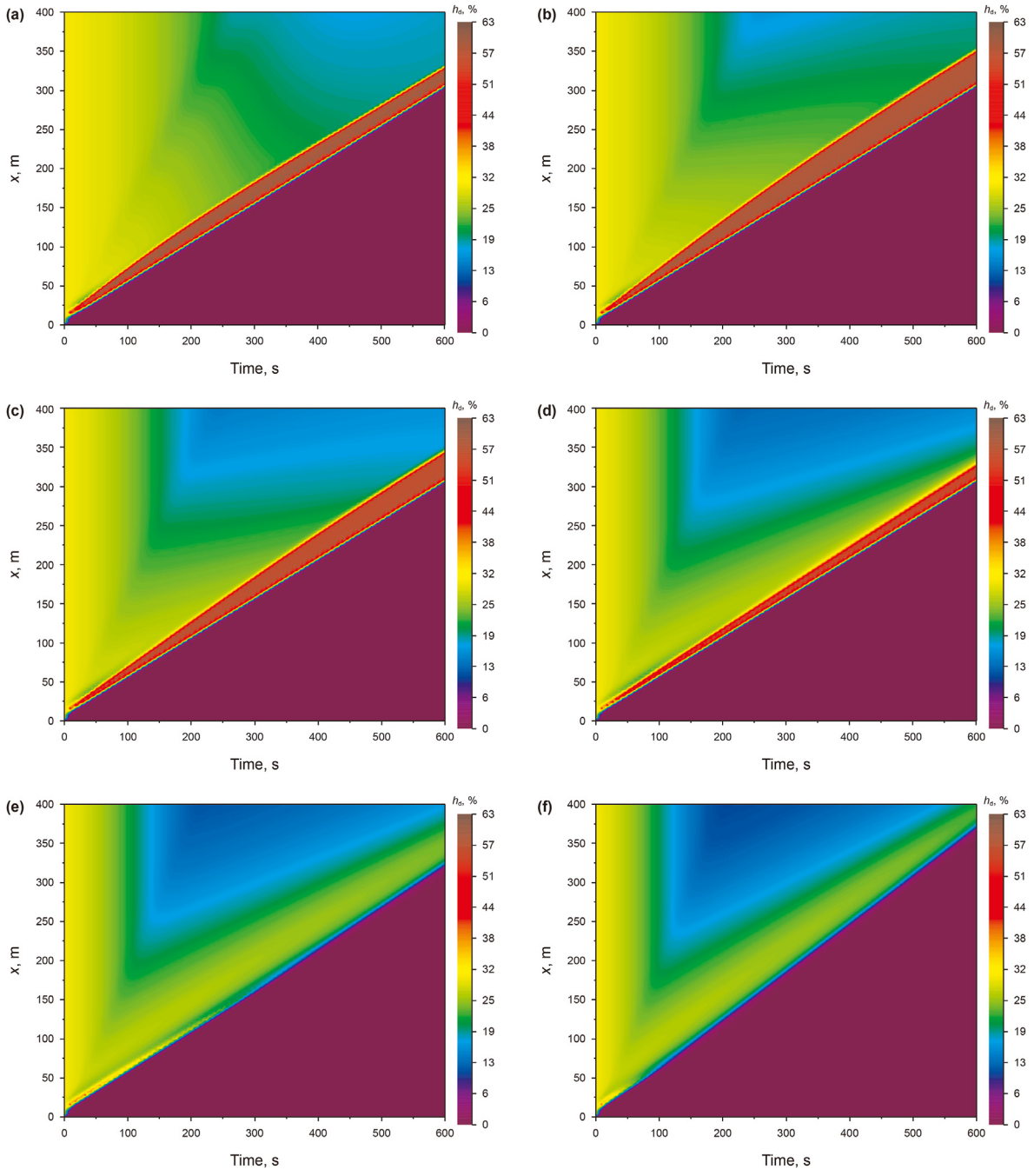

Fig. 21. Simulation results of different fluid flow rates: (**a**) 33 L/s; (**b**) 35.0 L/s; (**c**) 37.5 L/s; (**d**) 40.0 L/s; (**e**) 42.5 L/s; (**f**) 45 L/s.

considered in this study (Yarim et al., 2010), where the back-reaming operation is considered dangerous generally.

The drill pipe diameter and wellbore diameter change the cross-section area of the annulus, which has direct effects on the fluid velocity. With the drill pipe diameter increased, the average cuttings bed height with 0.5 m/s tripping velocities decreases and the "dangerous flow rate", "low flow rate", and "high flow rate" tend to decrease or have decreased, as shown in Fig. 29. The flow rate of 33 L/s falls within the interval of "low flow rate" for 0.13 or 0.14 m drill pipe diameter, but it is within the interval of "high flow rate" for 0.15 or 0.16 m drill pipe diameter. Through calculations, changes in wellbore diameter produce similar results. With the larger ratio of the drill pipe diameter to wellbore diameter applied, the critical flow rates between three intervals tend to decrease or have decreased.

When the fluid velocity increase with the decrease of the annulus cross-section area, the effect of "dangerous velocity" is gradually prone to attenuation, as shown in Fig. 30. When the inner pipe diameter is 0.145 m, the cuttings accumulation of 0.4 m/s is close to those of 0.8 and 1.0 m/s. Strictly speaking, the interval of "dangerous velocity" is still 0.4–0.5 m/s tripping velocities with inner pipe diameter less than 0.15 m, as shown in Fig. 30. With the increase of inner pipe diameter, the cuttings accumulation in annuli is reduced considerably under 0.4–0.5 m/s tripping velocities, but this effect is not so obvious under 0.8–1.0 m/s. The "dangerous velocity" is a relative concept. It can be found that the "dangerous

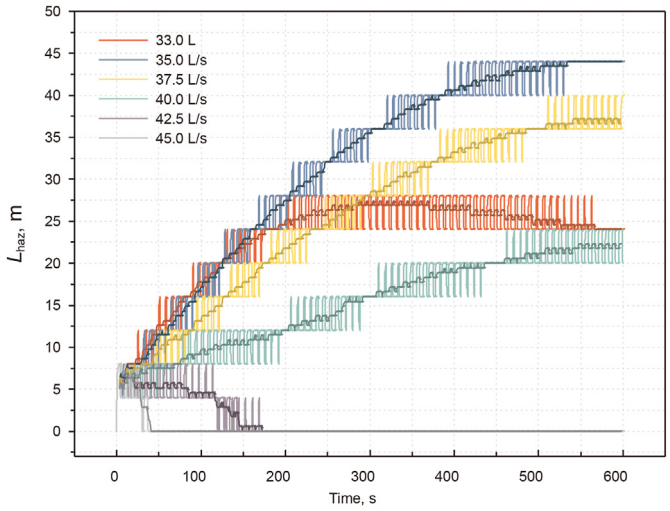

Fig. 22. The lengths of hazardous sections of different fluid flow rates.

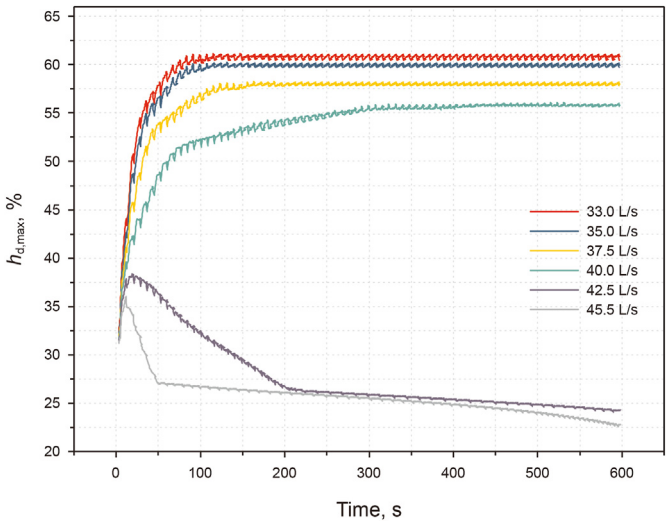

Fig. 24. The maximum dimensionless cuttings bed heights different fluid flow rates.

velocity" rises when conditions are more conducive to hole cleaning. As shown in Fig. 30, the interval of "dangerous velocity" is larger than 0.8–1.0 m/s, as the inner pipe diameter is 0.16 m. The interval of "dangerous velocity" is 0.5–1.0 m/s, when the inner pipe diameter is 0.155 m. This result is affected by the combination of fluid velocity and tipping velocity. Through calculations, changes in wellbore diameter produce similar results. With the larger ratio of the drill pipe diameter to wellbore diameter applied, the "dangerous velocity" tends to increase or has increased.

The bulldozer effect and cleaning effect of the bit in this model are not affected by particle properties and fluid properties directly. These conditions have effects on the cuttings' transport, entrainment, and deposition, which can lead to specific results. But the basic law of cuttings redistribution caused by the backreaming operations is similar to the conclusions in Section 4 through a lot of calculations. In brief, if the conditions are more favorable for hole cleaning, the "low flow rate", "high flow rate" and "dangers flow rate" tend to decrease and the "dangerous velocity" tends to increase. If hole cleaning declines, the opposite conclusions are obtained. Only the interactions between the flow rate and each of the properties of drilling fluid and particle are displayed below, which is enough to explain the effect of particle properties and fluid properties on the conclusions.

Table 9
Input parameters for Case 5.

Variables	Value	Unit
LSDT diameter	0.1788	m
Fluid flow rate	35	L/s
Initial cuttings bed height	30	%
LSDT length	4	m
Tripping velocity	0.2, 0.4, 0.5, 1.0	m/s

As shown in Fig. 31, the increase of particle diameter slightly reduces the cuttings bed height near the step surface under the given diameter range. The larger the particle diameter, the larger the bed roughness, the larger the interfacial friction coefficient, and the higher the transport efficiency of the cuttings bed. In addition, the increase of particle diameter makes the drag force get larger and increases too small resistance torque, which reduces the critical rolling velocity of a particle. However, the large particles would hinder hole cleaning when their diameters increase to a certain extent and too small cuttings is difficult to remove according to some previous studies (Duan et al., 2009; Nazari et al., 2010). In the one-dimensional cuttings transport model, the mass exchange flux depends on the critical rolling velocity, and the bed roughness is

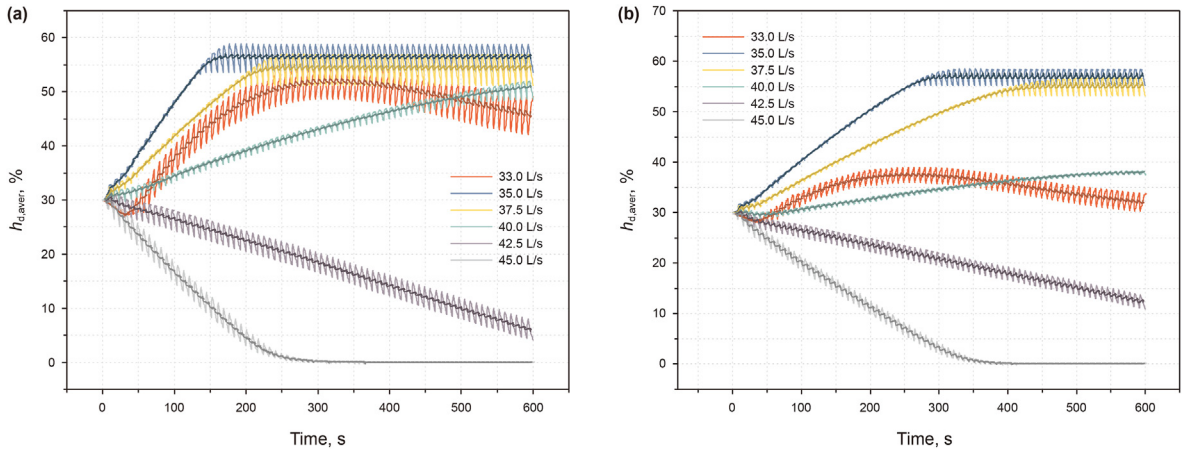

Fig. 23. The average dimensionless cuttings bed heights of different fluid flow rates: (**a**) 20 m above the step surface; (**b**) 40 m above the step surface.

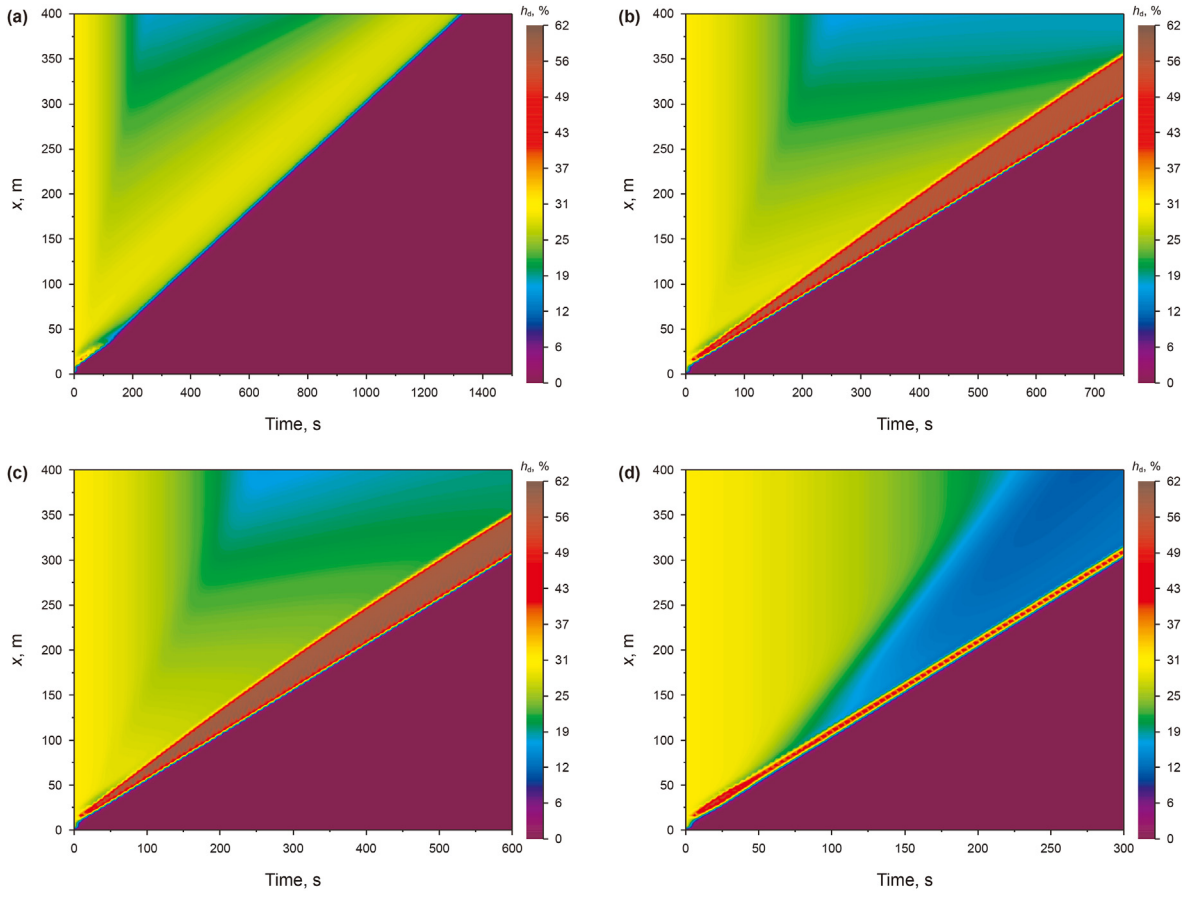

Fig. 25. Simulation results of different tripping velocities: (**a**) 0.2 m/s; (**b**) 0.4 m/s; (**c**) 0.5 m/s; (**d**) 1.0 m/s.

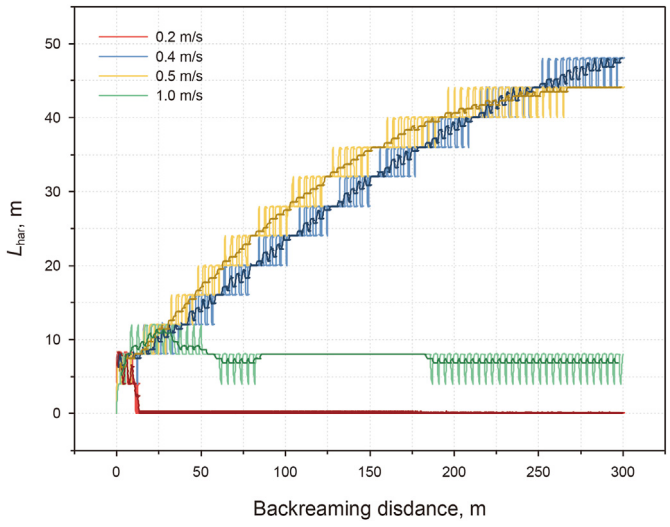

Fig. 26. The lengths of hazardous sections of different tripping velocities.

introduced, which makes the influence of single-particle gravity underestimated. Therefore, the one-dimensional model has certain limitations on the study of the effect of particle diameter and needs to be improved in later studies.

High particle density is not conducive to cuttings carried by drilling fluid, i.e. cuttings are more likely to settle into a cuttings bed due to the gravity, as the particle density increases. Moreover, the increase of particle density makes the dry friction force larger, which hinders the movement of the cuttings bed. As shown in Fig. 32, with the increase of particle density, the average cuttings bed height near the step surface increases, and the critical flow rate between the "low and high flow rate" interval increases.

The greater fluid density is generally beneficial for hole cleaning. Because higher drilling fluid density leads to stronger cuttings entrainment, *i.e.* the critical rolling rate decreases because of the increases of the buoyancy, drag force, and lift force. It is found that larger flow rates significantly improved the hole-cleaning effect of increased fluid density, as shown in Fig. 33.

The increase of consistency coefficient enhances the effective viscosity of drilling fluid, and it is beneficial to increase the interfacial friction factor. But a larger consistency coefficient increases the critical rolling velocity a little under these flow conditions. The combination of these two effects results in the following. With the increase of consistency coefficient, the cuttings bed height near the step surface decreases, but with the increase of the flow velocity, the decreasing trend is not obvious, as shown in Fig. 34.

The increase of yield strength implies a larger interfacial friction factor and larger effective viscosity of drilling fluid. And the larger yield strength makes cuttings' entrainment get larger. Increasing yield strength can improve the hole cleaning condition, as shown in Fig. 35. The drilling fluid conforming to the power-law model is not favorable to the hole cleaning under these flow conditions, because its yield strength is equal to or close to 0.

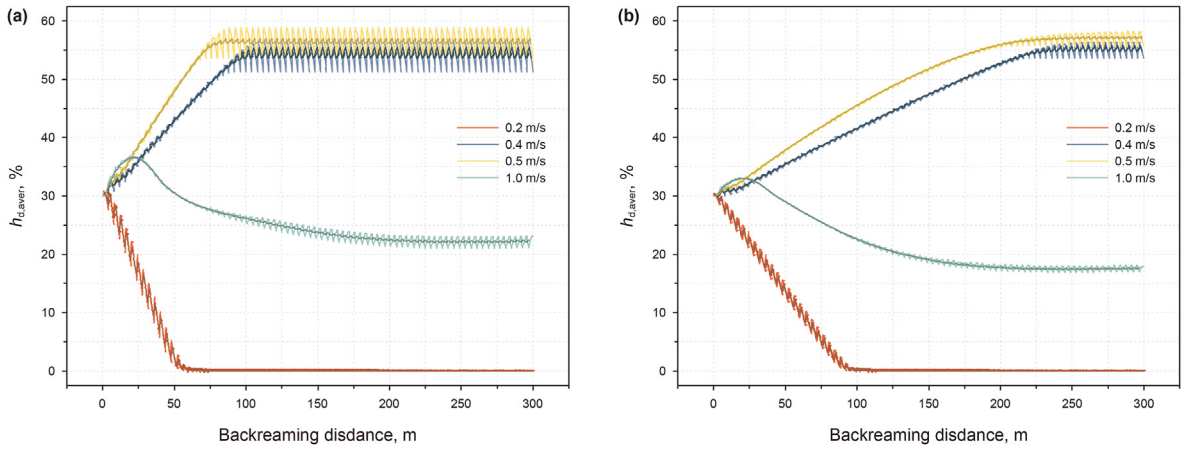

Fig. 27. The average dimensionless cuttings bed heights of different tripping velocities: (**a**) 20 m above the step surface; (**b**) 40 m above the step surface.

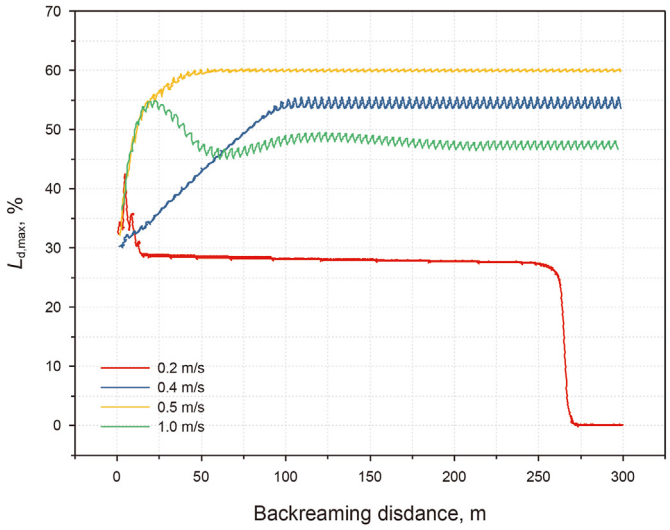

Fig. 28. The maximum dimensionless cuttings bed heights different tripping velocities.

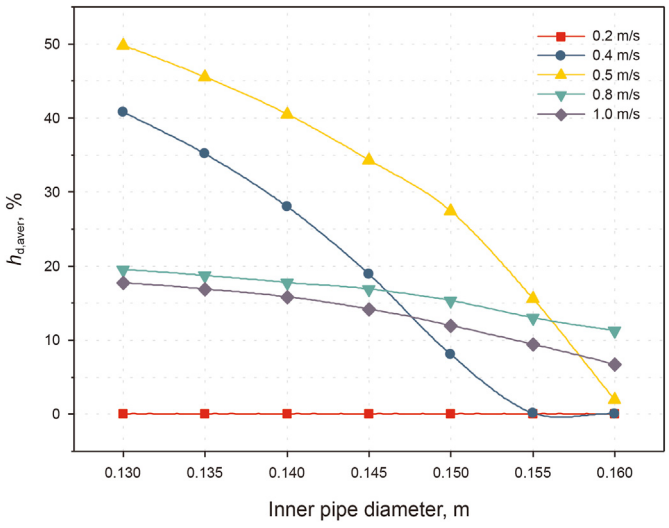

Fig. 30. Effect of inner pipe diameters on average dimensionless cuttings bed heights from 0 to 40 m from the LSDT for different tripping velocities.

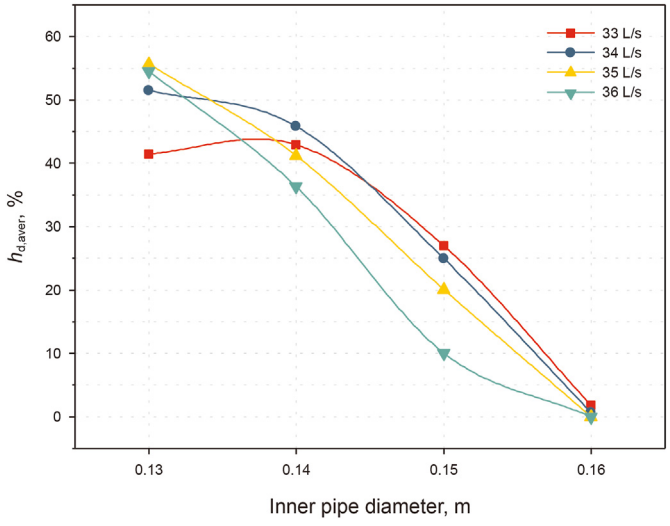

Fig. 29. Effect of inner pipe diameters on average dimensionless cuttings bed heights from 0 to 40 m from the LSDT for different flow rates.

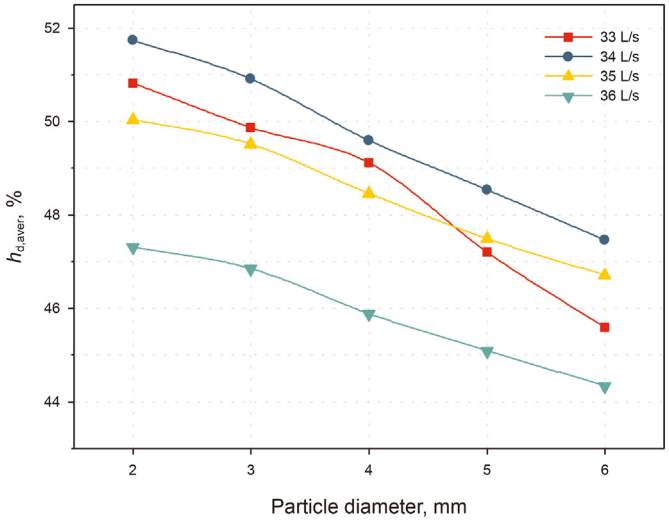

Fig. 31. Effect of particle diameters on average dimensionless cuttings bed heights from 0 to 40 m from the LSDT for different flow rates.

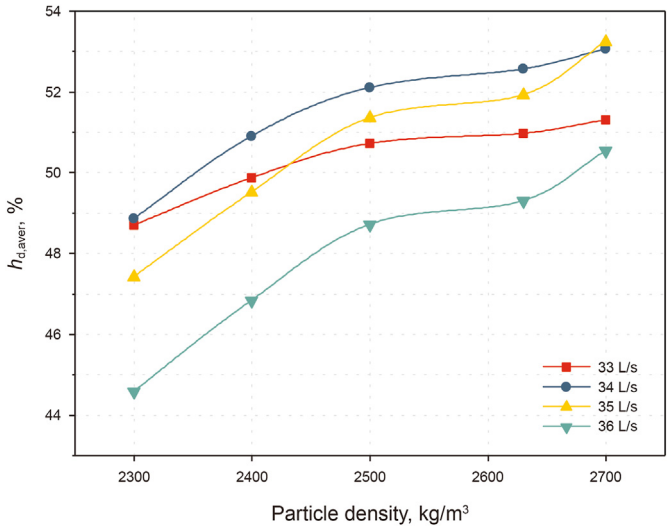

Fig. 32. Effect of particle density on average dimensionless cuttings bed heights from 0 to 40 m from the LSDT for different flow rates.

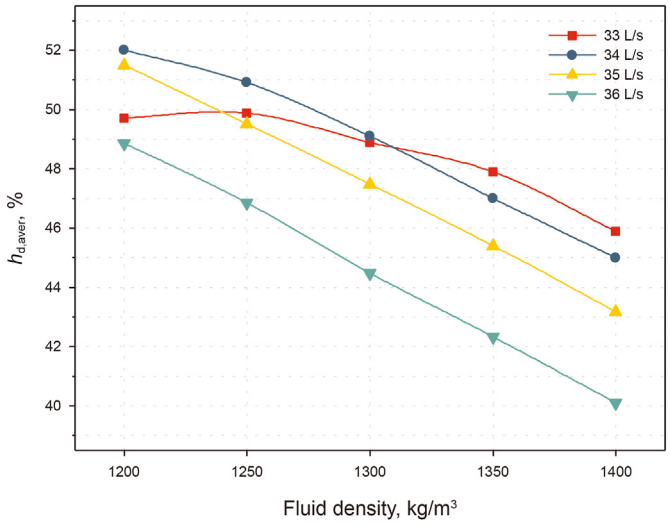

Fig. 33. Effect of fluid density on average dimensionless cuttings bed heights from 0 to 40 m from the LSDT for different flow rates.

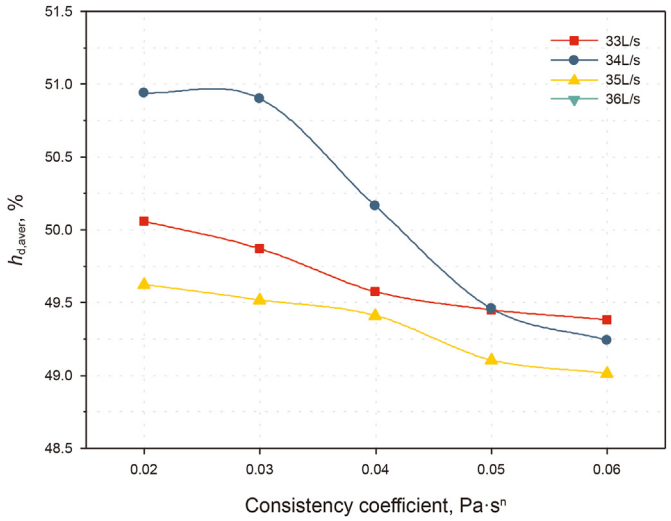

Fig. 34. Effect of consistency coefficient on average dimensionless cuttings bed heights from 0 to 40 m from the LSDT for different flow rates.

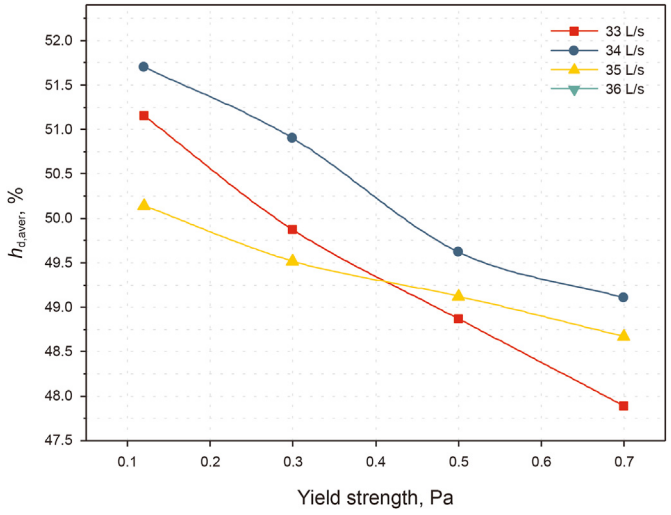

Fig. 35. Effect of yield strength on average dimensionless cuttings bed heights from 0 to 40 m from the LSDT for different flow rates.

6. Conclusions

(1) The conventional one-dimensional stratification model cannot meet the simulation needs for the backreaming process. A composite transient cuttings transport model considering five flow patterns is developed, and the predicted values in drilling conditions are in good agreement with experimental data within the error range ± 5%. The boundary conditions of the backreaming operation, unlike the conventional ones, are proposed, which are "bottom hole boundary", "clean boundary" and "reception boundary". The new model can satisfy the simulation of the whole process of the backreaming.

(2) A new theory to explain the cuttings transport while backreaming with LSDTs is proposed, in which the bit and LSDTs both have a "cleaning effect" and "plugging effect". The backreaming is a process of dynamic balance between the "cleaning effect" and "plugging effect".

(3) The length of the hazardous section, the average cuttings bed height near the step surface, and the maximum cuttings bed height are proposed to quantitatively describe the cuttings accumulation in the wellbore and serve as a basis for the risk of stuck pipe. The larger the diameter of the LSDT, the more severe the accumulation of cuttings bed in the wellbore due to the bulldozer effect, and the correlation is non-linear. The larger the length of the LSDT, the greater the risk of jams, which is mainly reflected in the length of the hazard section.

(4) It is not the case that a higher flow rate during the backreaming is better for borehole cleaning. The flow rate should be discussed in three intervals, which are from low to high including: "dangerous flow rate", "low flow rate" and "high flow rate". When the "dangerous flow rate" (<33 L/s in Case 4) is employed, the cuttings beds completely block the borehole near the step surface and directly cause a stuck pipe. When the flow rate is in the "low flow rate" interval (33–35 L/s in case 4), the risk level of jams increases with the increase of the flow rate. When the flow rate increases to the

"high flow rate interval" (>35 L/s in case 4), the higher the flow rate the cleaner the borehole is.

(5) For the tripping velocity, there is an interval called the "dangerous velocity", in which more cuttings beds are deposited near the LSDTs obviously than those of other velocities. Theoretically, as long as the applied tripping velocity is not within the "dangerous velocity" interval (0.4–0.5 m/s in Case 5), the risk of the stuck pipe can be controlled validly.

(6) Fluid properties, particle properties, and annular geometry have effects on the cuttings' transport, entrainment, and deposition, which can affect specific results. But the basic law of cuttings redistribution caused by the backreaming operations remains consistent. In brief, if the conditions are more favorable for hole cleaning, the "low flow rate", "high flow rate" and "dangers flow rate" tend to decrease and the "dangerous velocity" tends to increase. If hole cleaning declines, the opposite conclusions are reached.

In conclusion, the redistribution of the cuttings bed due to the backreaming operation should be quantitatively evaluated to lower the risk of the stuck pipe. Real-time simulation of the backreaming operation is crucial for parameters' setting and adjustment. The research of this paper is aimed at assisting the design and implementation of the backreaming.

Declaration of competing interest

The authors declare that they have no known competing financial interests or personal relationships that could have appeared to influence the work reported in this paper.

Acknowledgments

The authors gratefully acknowledge the National Natural Science Foundation of China, China (Grant No. 52227804, 52174010), Strategic Cooperation Technology Projects of CNPC and CUPB, China (Grant No. ZLZX2020-01), Sinopec key laboratory of drilling completion and fracturing of shale oil and gas, China (Grant No. 35800000-22-ZC0699-0004), the Key Projects of Scientific Research Plan in Colleges and Universities of Xinjiang Uygur Autonomous Region, China (Grant No. XJEDU20211028).

Appendix A. Closure relationships

The solids and liquids fill the suspension layer, as shown in Eq. (A-1).

$$C_f + C_c = 1 \tag{A-1}$$

The density of the cuttings bed is expressed as:

$$\rho_{sb} = \rho_c C_{sb} + \rho_f (1 - C_{sb}) \tag{A-2}$$

Shear stresses for each phase at the pipe wall can be expressed as:

$$\tau_i = \frac{1}{2} f_i \rho_i v_r^2 \tag{A-3}$$

where i represents fw, cw, sbw; v_r represents the relative velocity between the phase and the wall of pipe or borehole. f_i is the friction factor proposed by Doron et al. (1987).

$$f_i = \begin{cases} \dfrac{16}{Re_{gn}} & Re_{gn} \leqslant 3470 - 1370n \\ 0.046 Re_{gn}^{-0.2} & Re_{gn} > 3470 - 1370n \end{cases} \tag{A-4}$$

Shear stress at the interface between two layers is:

$$\tau_{sbsd} = \frac{1}{2} f_{sbsd} \rho_f \left| v_f - v_{sb} \right| \left(v_f - v_{sb} \right) \tag{A-5}$$

where f_{sbsd} is the interfacial friction factor (Bizhani and Kuru, 2018). For a turbulent flow, this interfacial friction factor model is within the 20% range of experimental data (Bizhani and Kuru, 2018). It has higher accuracy than the Televantos et al. (1979) model.

$$\begin{cases} f_{sbsd} = \dfrac{16}{Re_{gn}} & Re_{gn} \leqslant 2100 \\ \dfrac{1}{\sqrt{f_{sbsd}}} = -4 \log \left(\dfrac{0.27 \varepsilon_b}{D_{hy}} + \dfrac{1.26}{Re_{gn} f_{sbsd}^{1/2}} \right) & Re_{gn} > 2100 \end{cases} \tag{A-6}$$

Bed roughness can be expressed as:

$$\varepsilon_b = \frac{d_c}{2} (1 + \sin \varphi) \tag{A-7}$$

where φ is the reposed angle.

The generalized Reynolds number for the Herschel-Bulkley model suggested by Tong et al. (2021a) is expressed as:

$$Re_{gn}(\rho, v, D) = \frac{\rho |v|^{2-n} D^n}{\frac{\tau_y}{8} \left(\frac{D}{v} \right)^n + K \left(\frac{3m+1}{4m} \right)^n 8^{n-1}} \tag{A-8}$$

$$m = \frac{nK(8v/D)^n}{\tau_y + K(8v/D)^n} \tag{A-9}$$

F_{cf} represent multiparticle-drag force between the particles and the liquids (Tong et al., 2021a; Chen et al., 2022).

$$F_{cf} = C_c A_{sd} \frac{3 C_D \rho_f \left| v_f - v_c \right| \left(v_f - v_c \right)}{4 d_c (1 - C_c)^{1.65}} \tag{A-10}$$

where the drag coefficient can be expressed (Naganawa et al., 2017):

$$C_D = \begin{cases} \dfrac{24}{Re_p} \left(1 + 0.15 Re_p^{0.687} \right) & Re_p < 1000 \\ 0.44 & Re_p \geqslant 1000 \end{cases} \tag{A-11}$$

$$Re_p = Re_{gn} \left(\rho_f, v_f - v_c, d_c \right) \tag{A-12}$$

The dry friction force F is the kinetic friction force between the moving bed and the hole wall suggested by Nawanaga et al. (2017).

The wetted perimeters (S_{sd}, S_{sb}, S_{sbsd}) can be obtained by geometric calculations (Zhu et al., 2021).

References

Aitken, B., Li, J., 2013. Solids Cleanout Analysis Reduces Screen Out Risk. SPE/ICoTA Coiled Tubing & Well Intervention Conference & Exhibition. OnePetro, Woodlands, Texas, USA. https://doi.org/10.2118/163895-MS.

An, J., Li, J., Huang, H., Liu, G., Yang, H., Zhang, G., Chen, S., 2023. Transient cutting transport model for horizontal wells with a slim hole. Energy Sci. Eng. 11 (2),

796–810. https://doi.org/10.1002/ese3.1363.
Bizhani, M., Kuru, E., 2018. Critical review of mechanistic and empirical (semi-mechanistic) models for particle removal from sandbed deposits in horizontal annuli with water. SPE J. 23 (2), 237–255. https://doi.org/10.2118/187948-PA.
Chen, Y., Zhang, H., Li, J., Zhou, Y., Lu, Z., Ouyang, Y., Zhang, G., 2022. Simulation study on cuttings transport of the wavy wellbore trajectory in the long horizontal wellbore. J. Petrol. Sci. Eng. 110584. https://doi.org/10.1016/j.petrol.2022.110584.
Doron, P., Granica, D., Arnea, D., 1987. Slurry flow in horizontal pipes—experimental and modeling. Int. J. Multiphas. Flow 13 (4), 535–547. https://doi.org/10.1016/0301-9322(87)90020-6.
Duan, M., Miska, S.Z., Yu, M., Takach, N.E., Ahmed, R.M., Zettner, C.M., 2009. Critical conditions for effective sand-sized solids transport in horizontal and high-angle wells. SPE Drill. Complet. 24 (2), 229–238. https://doi.org/10.2118/106707-PA.
Epelle, E.I., Gerogiorgis, D.I., 2018. CFD modeling and simulation of drill cuttings transport efficiency in annular bends: effect of particle sphericity. J. Petrol. Sci. Eng. 170, 992–1004. https://doi.org/10.1016/j.petrol.2018.06.041.
Fan, Y., Tian, Z., Ming, R., Yang, H., Fu, L., Wang, Y., Guo, K., 2020. Research on horizontal wellbore cleaning monitoring technologies. Chin. Petrol. Mach. 48 (3), 1–9. https://doi.org/10.16082/j.cnki.issn.1001-4578.2020.03.001 (in Chinese).
Gavignet, A.A., Sobey, I.J., 1989. Model aids cuttings transport prediction. J. Petrol. Technol. 41 (9), 916–921. https://doi.org/10.2118/15417-PA.
Khaled, M.S., Khan, M.S., Ferroudji, H., Barooah, A., Rahman, M.A., Hassan, I., Hasan, A.R., 2021. Dimensionless data-driven model for optimizing hole cleaning efficiency in daily drilling operations. J. Nat. Gas Sci. Eng. 96. https://doi.org/10.1016/j.jngse.2021.104315.
Khatibi, M., Time, R.W., Shaibu, R., 2018. Dynamical feature of particle dunes in Newtonian and shear-thinning flows: relevance to hole-cleaning in pipe and annulus. Int. J. Multiphas. Flow 99, 284–293. https://doi.org/10.1016/j.ijmultiphaseflow.2017.10.015.
Mahaffy, J.H., 1982. A stability-enhancing two-step method for fluid flow calculations. J. Comput. Phys. 46 (3), 329–341. https://doi.org/10.1016/0021-9991(82)90019-5.
Naganawa, S., Nomura, T., 2006. Simulating Transient Behavior of Cuttings Transport over Whole Trajectory of Extended Reach Well. IADC/SPE Asia Pacific Drilling Technology Conference and Exhibition. OnePetro, Bangkok, Thailand. https://doi.org/10.2118/103923-MS.
Naganawa, S., Sato, R., Ishikawa, M., 2017. Cuttings-transport simulation combined with large-scale-flow-loop experimental results and logging-while-drilling data for hole-cleaning evaluation in directional drilling. SPE Drill. Complet. 32 (3), 194–207. https://doi.org/10.2118/171740-PA.
Nazari, T., Hareland, G., Azar, J.J., 2010. Review of Cuttings Transport in Directional Well Drilling: Systematic Approach. SPE Western Regional Meeting. OnePetro, Anaheim, California, USA. https://doi.org/10.2118/132372-MS.
Sun, Y., Jia, L., 2020. Cases and understandings on the drilling of horizontal well with horizontal section of 3000 m long in China. Oil Drill. Product. Technol. 42 (4), 393–401. https://doi.org/10.13639/j.odpt.2020.04.002 (in Chinese).
Tan, T., Zhang, H., 2022. A risk prediction method of pipe sticking accidents due to wellbore uncleanness for long horizontal section wells. J. Petrol. Sci. Eng. 210, 110023. https://doi.org/10.1016/j.petrol.2021.110023.
Televantos, Y., Shook, C., Streat, M., Carleton, A., 1979. Flow of slurries of coarse particles at high solids concentrations. Can. J. Chem. Eng. 57 (3), 255–262. https://doi.org/10.1002/cjce.5450570302.
Tong, T.A., Ozbayoglu, E., Liu, Y., 2021a. A transient solids transport model for solids removal evaluation in coiled-tubing drilling. SPE J. 1–18. https://doi.org/10.2118/205370-PA.
Tong, T.A., Liu, Y., Ozbayoglu, E., Yu, M., Ettehadi, R., May, R., 2021b. Threshold velocity of non-Newtonian fluids to initiate solids bed erosion in horizontal conduits. J. Petrol. Sci. Eng. 199, 108256. https://doi.org/10.1016/j.petrol.2020.108256.
Wang, X., 2020. Modeling and Analysis Research of Dynamic Cuttings Transport in Extended Reach Well. Yangtze University (in Chinese).
Wang, Z.M., Long, Z.H., 2010. Study on three-layer unsteady model of cuttings transport for extended-reach well. J. Petrol. Sci. Eng. 73 (1–2), 171–180. https://doi.org/10.1016/j.petrol.2010.05.020.
Yarim, G., Ritchie, G.M., May, R.B., 2010. A guide to successful backreaming: real-time case histories. SPE Drill. Complet. 25 (1), 27–38. https://doi.org/10.2118/116555-PA.
Yarim, G., Uchytil, R.J., May, R.B., Trejo, A., 2007. Stuck Pipe Prevention–a Proactive Solution to an Old Problem. SPE Annual Technical Conference and Exhibition, Anaheim. OnePetro, Californi, USA. https://doi.org/10.2118/109914-MS.
Zhu, N., Huang, W., Gao, D., 2022. Numerical analysis of the stuck pipe mechanism related to the cutting bed under various drilling operations. J. Petrol. Sci. Eng. 208, 109783. https://doi.org/10.1016/j.petrol.2021.109783.
Zhang, F., 2015. Numerical Simulation and Experimental Study of Cuttings Transport in Intermediate Inclined Wells. The University of Tulsa.
Zhang, F., Miska, S., Yu, M., Ozbayoglu, E., 2018. A unified transient solid-liquid twophase flow model for cuttings transport-modelling part. J. Petrol. Sci. Eng. 166, 146–156. https://doi.org/10.1016/j.petrol.2018.03.027.
Zhang, F., Wang, Y., Wang, Y., Miska, S., Yu, M., 2020. Modeling of dynamic cuttings transportation during drilling of oil and gas wells by combining 2D CFD and 1D discretization approach. SPE J. 25 (3), 1220–1240. https://doi.org/10.2118/199902-PA.
Zamora, M., Jefferson, D.T., Powell, J.W., 1993. Hole Cleaning Study of Polymer-Based Drilling Fluids. SPE Annual Technical Conference and Exhibition, Houston, USA. https://doi.org/10.2118/26329-PA.
Zhu, N., Huang, W., Gao, D., 2021. Dynamic wavy distribution of cuttings bed in extended reach drilling. J. Petrol. Sci. Eng. 198, 108171. https://doi.org/10.1016/j.petrol.2020.108171.